DOI: 10.1002/smll.200700064

Self-Repairing Coatings Containing Active Nanoreservoirs

*Dmitry G. Shchukin and Helmuth Möhwald**

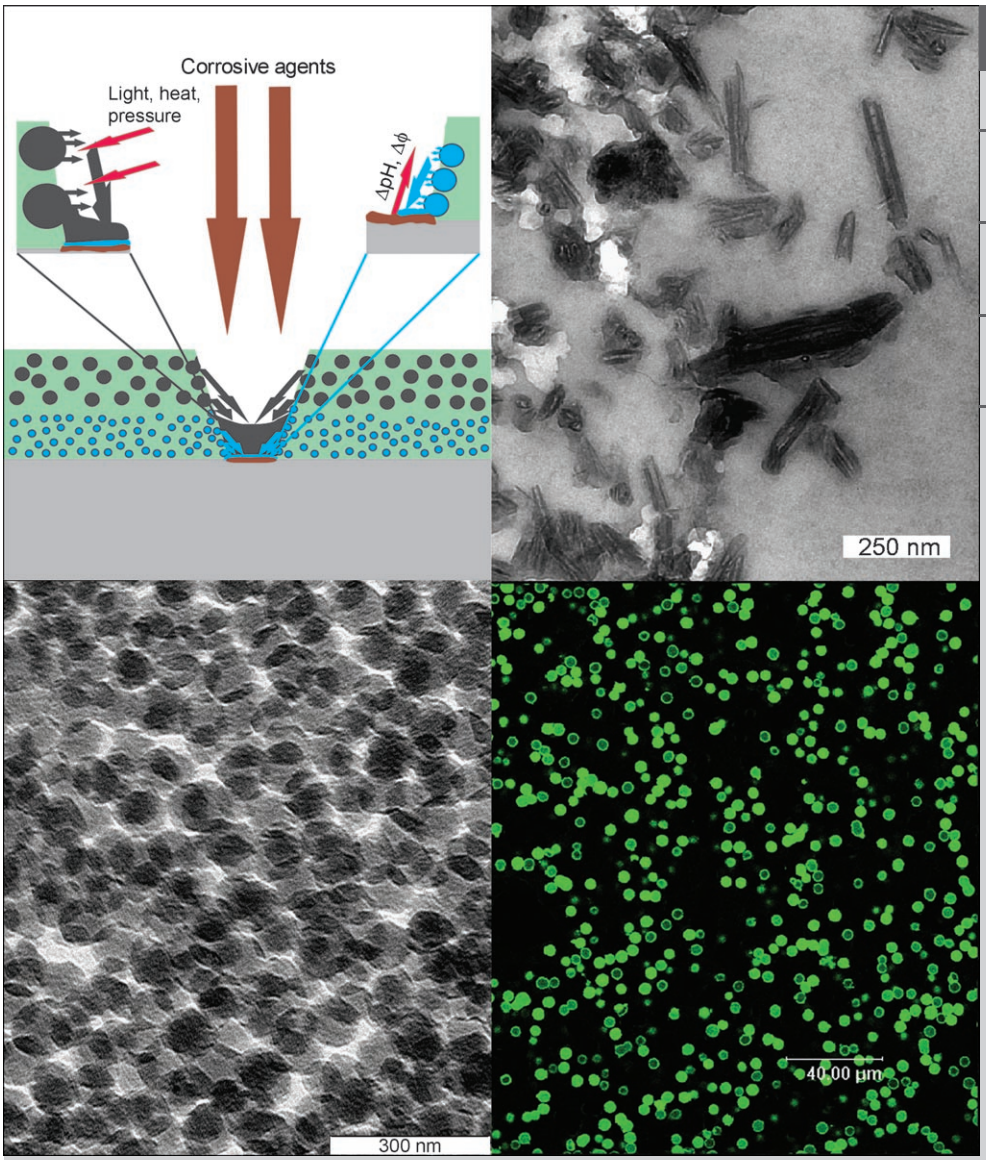

Small containers with encapsulated materials pave the way for novel self-repairing coatings with applications in many arenas.

NANO MICRO small

From the Contents

Keywords:
- anticorrosion coatings
- capsules
- nanocontainers
- self-healing
- self-repairing

small NANO MICRO

Nanocontainers with the ability to release encapsulated active materials in a controlled way can be employed to develop a new family of self-repairing multifunctional coatings, which possess not only passive functionality but also rapid feedback activity in response to changes in local environment. Several approaches to fabricate self-repairing coatings on plastic and metal substrates were surveyed. The release of the active materials occurs only when triggered, which prevents leakage of the active component out of the coating and increases coating durability. This Review also covers some principles and recent developments in the fabrication of nanocontainers with good compatibility with the coating components, the possibility to encapsulate and upkeep active material, and permeability properties of the shell controlled by external stimuli. Depending on the nature of the sensitive components introduced into the container shell, reversible and irreversible changes of the shell permeability can be induced by various stimuli. Different responses can be then observed varying from fine effects like tunable permeability to more drastic ones like total rupture of the container shell.

1. Introduction

Development of a new generation of self-repairing coatings and bulk materials, which have both passive mechanical characteristics originated from matrix material and active response sensitive to changes in the local environment or to the integrity of the passive matrix, opens an avenue for the fabrication of future high-tech functional surfaces. Novel feedback-active surfaces can be composed of a passive matrix inherited from a "classical" approach for coatings and active structures for fast response of the coating properties to outer environmental impacts. Corrosion losses are one of the important destruction processes to be prevented by active surfaces to reduce the depreciation of investments and to increase the security of ground and air transportation. Active corrosion protection aims to decrease the corrosion rate when the main barrier (main coating matrix) is damaged and corrosive species come into contact with the substrate.[1,2]

The coatings have to provide release of the active and repairing material rapidly after changes in coating integrity. The active agents (e.g., corrosion inhibitors) can be introduced in the different components of the coating: pretreatment, primer, and topcoat. The agents are effective only if their solubility in the defect environment is in the right range. Very low solubility leads to lack of active agent at the substrate interface and consequently to weak feedback activity. If the solubility is too high the substrate will be protected, but for only a relatively short time since the active agent will be rapidly leached out from the coating. Another drawback, which can appear due to high solubility, is the osmotic pressure that leads to blistering and delamination of the active surface. The osmotic pressure can stimulate water to be transported through the coating, which acts as a semipermeable membrane, causing the destruction of the passive matrix.

Recent developments in surface science and technology offer new opportunities for modern engineering concepts for the fabrication of active surfaces of the "passive" host–"active" guest structure through either the fabrication of active composite-layered systems in which the passive coating matrix is alternated with layers bearing an active coating component (e.g., inhibitor, lubricant) or the integration of nanoscale containers (carriers) loaded with the active components into existing "classical" coatings (Figure 1a,b). The first approach (Figure 1a) involves doping the passive matrix with active components, which are released upon environmental triggering (some examples of this approach are described below).[3] However, interaction of the active materials with the passive matrix leads to significant shortcomings in the stability and self-repairing activity of the coating. Moreover, free inhibitor inside the active matrix is often subjected to spontaneous leakage from the surface during aging. The rate of release of the active load is dependent on the structural, chemical, and acidic/alkaline properties of the passive matrix.[4]

The main idea of the second approach is to load active compounds into nanocontainers with a shell possessing con-

[*] Dr. D. G. Shchukin, Prof. Dr. H. Möhwald
Max-Planck Institute of Colloids and Interfaces
14424 Potsdam (Germany)
Fax: (+49) (0)331-567-9202
E-mail: dmitry.shchukin@mpikg.mpg.de

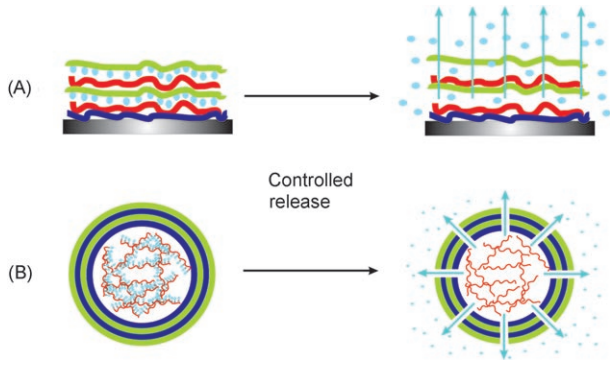

Figure 1. Schematic illustration of the entrapment/release of active materials. A) Active material is embedded in the "passive" matrix of the coating; B) active material is encapsulated into nanocontainers with a shell possessing controlled permeability properties.

trolled permeability (Figure 1b) and then to introduce them into the coating matrix. As a result, nanocontainers are uniformly distributed in the passive matrix keeping active material in a "trapped" state, thus avoiding the undesirable interaction between the active component and the passive matrix, leading to spontaneous leakage. When the local environment undergoes changes or if the active surface is affected by the outer impact, the nanocontainers respond to this signal and release encapsulated active material.

The most important task for the second approach is to develop nanocontainers with good compatibility with the matrix components, the possibility to encapsulate and upkeep active material, and control of the permeability properties of the shell thorugh external stimuli. The nanocontainers should also be of a size less than 300–400 nm; nanocontainers of larger size can damage the integrity of the coating matrix forming large hollow cavities, which reduce the passive protective properties of the coating. Depending on the nature of the sensitive components (e.g., weak polyelectrolytes, metal nanoparticles) introduced into the container shell, reversible and irreversible changes of the shell permeability can be induced by various stimuli: variation of the pH, ionic strength, temperature, ultrasonic treatment, alternating magnetic field, electromagnetic irradiation. Different responses can then be observed, varying from fine effects such as tunable permeability to more drastic ones like total rupture of the container shell.[5]

Several approaches have been developed to date to fabricate micro- and nanocontainers.[6] One approach is based on the self-assembly of lipid molecules or amphiphilic block copolymers into spherically closed bilayer structures (vesicles).[7,8] These relatively unstable structures can undergo crosslinking to stabilize the nanocontainer shell. A second approach is to use dendrimers or hyperbranched polymers as nanocontainers.[9,10] However, the particle preparation is a rather costly and time-consuming procedure limiting possible applications and up-scaling. A third method involves the layer-by-layer assembly of oppositely charged species on the outermost surface of dense template nanoparticles using polyelectrolytes, conductive polymers, biopolymers, carbon nanotubes, viruses, lipid vesicles, and nanoparticles as constituents of the nanocontainer shell.[11] A fourth approach involves the use of ultrasonic waves to fabricate inorganic and composite hollow nanospheres.[12] In this case, a cavitation interface is employed as a reaction zone where a sensitive shell is formed from organic precursors or preformed nanoparticles adsorbed at the gas/liquid interface via polycondensation, polymerization, and particle melting (or sonoinduced welding). Ultrasonic synthesis can result in hollow spheres containing either gas or liquid in their inner cavity. Finally, a fifth procedure involves suspension and emulsion polymerization around latex particles. This method is well studied and out of the scope of this review. For more detailed information on the fabrication of hollow containers by polymerization methods we refer to several recent reviews.[13,14]

2. Fabrication of Nanocontainers

In general, research on nanocontainer formation and loading requires the ability to form a nanocontainer shell, which should be stable, permeable (to release/upload mate-

Dmitry Shchukin is currently working at the Max Planck Institute of Colloids and Interfaces, Potsdam, Germany. He obtained his PhD (2002) in physical chemistry. He was an Alexander von Humboldt fellow, and a Marie-Curie fellow at the Max Planck Institute of Colloids and Interfaces (2001–2002, 2004–2005, 2005–2007), an INTAS fellow at the Ecole Centrale de Lyon, France (2001), and a postdoctoral research fellow at the Louisiana Tech University, Ruston, USA (2002–2003). He was awarded the NanoFutur Prize from the German Ministry of Education and Research in 2006. His main scientific interests concern the fabrication of hollow nanocontainers, study of the chemical and physicochemical processes in confined nanoenvironments, interfacial sonochemistry, and feedback-active coatings.

Helmuth Möhwald is currently a director at the Max Planck Institute of Colloids and Interfaces heading the department "Interfaces". He is also honorary professor at the University of Potsdam and guest professor at Fudan and Zheijang Universities, China. He previously held a chair in physical chemistry at the University of Mainz (1987–1993) and was associate professor of biophysics at TU Munich (1981–87). He also spent five years in industry (IBM San Jose 1974–75 and Dornier-Systems 1978–1981). Among his recognitions are the physics award of the German Physical Society (1978), the Liesegang award of the Kolloidgesellschaft (1998), and membership of the Austrian Academy of Sciences. His research interests include molecular interfaces, coated colloids and capsules, membranes, and chemistry and physics in confined volumes.

NANO MICRO small

rials), and should also possess other desired functionalities (magnetic, catalytic, conductive, targeting, etc.). In order to develop functionalized micro- and nanocontainers, one has to combine several properties in the shell structure and composition. Depending on the nature of the "smart" components introduced in the container shell, various stimuli can induce reversible and irreversible shell modifications. Different responses can be found, as described above.

In this section, we overview the most promising procedures for the fabrication of nanosized containers loaded with active materials, which can be used as components of the active surface: self-assembly of lipids and block copolymers, ultrasonically induced self-assembly, and alternating layer-by-layer adsorption of oppositely charged species (LbL assembly).

2.1. Self-Assembled Nanocontainers

Self-organizing block copolymers and lipid nanocontainers can entrap hydrophobic active materials within their core, while the outer shell confers water solubility. The ratio between the blocks and the concentration of the polymer influences the aggregation of block copolymers into vesicles, spheres, lamellae, rods, and other related structures (Figure 2).[15] It is possible to induce a transition between aggregate structures by slight perturbations of any given system.[16] The sizes of nanocontainers can be controlled by the molecular weight of the polymer and the ratio between the block sizes.[17] Combining the block-copolymer nanocontainers with the entrapment of active materials opens a new area of fabrication of active surfaces, especially for nonaqueous media.

Several amphiphilic block copolymers have been investigated as components of the nanocontainers, for example, poly(ethylene oxide), poly(*N*-isopropyl acrylamide), polypyrrolidones; biodegradable polymers such as poly(caprolactone), poly(D,L-lactide), or poly(D,L-lactic acid-*co*-glycolic acid). "Intelligent" nanocontainer vehicles can be designed by utilizing stimuli-responsive polymers that are sensitive to changes in temperature or pH value.[18,19] Poly(*N*-isopropyl acrylamide) undergoes a phase transition at 32 °C and can be used to fabricate thermosensitive nanocontainers. pH-sensitive micelles are usually prepared from double-hydrophilic block copolymers, which can be dissolved in water at a certain pH value and aggregate spontaneously upon an appropriate change in the pH value. Crosslinking of the shell components is often used to stabilize the hollow structures of block-copolymer containers. Typical crosslinking methods involve the polymerization of macromonomers with amphiphilic block structures in their side chain or the attachment of polymerizable groups along the hydrophobic block, or to fix0 the shell after aggregation of the block copolymers in aqueous solution.[20] Unfortunately, crosslinking decreases the capacity of the inner volume.

Nanocontainers with dimensions of ≈50 nm prepared from the micellar aggregation of diblock copolymers of poly(ethylene oxide) and polycaprolactone were explored as a carrier system for water-soluble materials.[21] The nanocontainers exhibited a loading efficiency of 38 % in a 1 % (w/v) nanocontainer solution. Release from the nanocontainers proceeded in a linear fashion for a duration of about 4–7 days depending on the composition of the block copolymers. Hollow carbonaceous capsules with a reactive surface layer and a tunable void size and shell thickness were prepared through a hydrothermal method at 180 °C using only the anionic surfactant sodium dodecyl sulfate and glucose as the starting materials.[22] The process is green, cheap, and easy. Samples showed tunable void sizes (50 nm–3 μm), thickness (10–300 nm), and appearance (spherical, apple-like, or bowl-like). Optically addressable microcapsules were prepared combining a photochemical approach and self-assembly.[23] Chlorobenzyl-functionalized poly-(organosiloxane) nanoparticles were introduced in a water/oil/water emulsion and their photochemical crosslinking was performed using a 200 W Hg–Xe lamp for several hours. The inner aqueous void contained cyclodextrin. The thickness, mechanical stability, and light resistance of the container walls could be controlled by regulating the number of photoreactive chlorobenzyl-functionalized poly-(organosiloxane) nanoparticles in the shell. These nanocontainers can be destroyed by photocleavage.

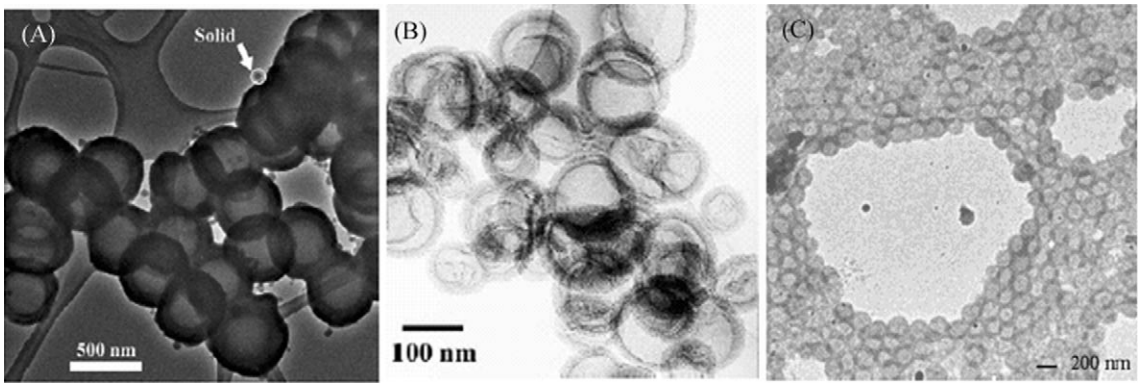

Figure 2. A) Transmission electron microscopy (TEM) image of polystyrene mesoporous shells (reprinted from Ref. [15b]. Copyright, American Chemical Society); B) TEM image of organosilica hollow shells (reprinted from Ref. [15c]. Copyright, American Chemical Society); C) TEM image of polyelectrolyte stimuli-responsive nanocontainers (reprinted from Ref. [37]).

Hollow silica nanospheres of controllable size can be made with Lys:Phe 1:1 block copolypeptides, whereas at higher block ratios, dense silica nanospheres are formed.[24] Hollow titania microspheres ranging from 100 nm to a few micrometers in diameter were synthesized using surfactant-stabilized nonaqueous nanodroplets.[25] Well-defined hollow spheres with amorphous titania walls were prepared by the addition of water to formamide dispersions of hexadecane droplets containing titanium ethoxide. Hydrolysis/condensation reactions at the formamide/oil interface gave rise to intact shells that could have application as low-density pigments, in self-repairing coatings, and photoactive storage/release agents. Similarly, colloidal suspensions of titania nanosheets were assembled into hollow shells using a layer-by-layer polyelectrolyte-mediated deposition.[26] Unilamellar and multilamellar silica colloids have been synthesized using surfactant vesicles or by the spray-drying of reaction solutions containing cationic surfactant templates.[27] Hollow shells with thin walls of amorphous silica or ordered mesostructured silica were prepared by sol–gel reactions at the surface of oil droplets containing tetraethoxysilane dispersed in aqueous reaction solutions.[28]

2.2. Layer-by-Layer-Assembled Containers

Layer-by-layer (LbL) assembly of oppositely charged species was first proposed by Iler in 1966 and later developed by Mallouk et al. and Decher et al. implementing polycations, polyanions, and charged nanoparticles as the constituents of the container shell.[29] The procedure of nanocontainer construction consists of the templating of LbL-assembled films on the surface of micrometer and submicrometer-sized colloidal particles.[30,31] Polyelectrolytes or other charged species alternately adsorb on the surface of the template particle recharging it. After washing out the excess of the deposited species, the composites are then mixed with oppositely charged material, so that the surface recharges again. By repeating the cycle, a multilayer shell can be obtained. The universal character of the method does not have any restriction on the type of the charged species employed for shell construction. The layer-by-layer deposition method has been used for more than 50 various charged macromolecules including synthetic polyelectrolytes, conductive polymers and biopolymers (proteins and nucleic acids), carbon nanotubes, viruses, lipid vesicles, and nanoparticles (e.g., Fe_3O_4, CdSe). The precision of one adsorbed layer thickness is about 1 nm. Core decomposition leads to the formation of hollow structures whose size and shape is determined by the initial colloidal core and the shell, which is composed of multilayers that are tunable in the nanometer range (Figure 3).

The shell of the resulting polyelectrolyte capsules is semipermeable and sensitive to a variety of physical and chemical conditions of the surrounding media, which might dramatically influence the structure of the polyelectrolyte complexes. High-molecular-weight compounds are excluded by the polyelectrolyte shell whilst small molecules, such as dyes and ions, can readily penetrate the capsule wall.[32,33]

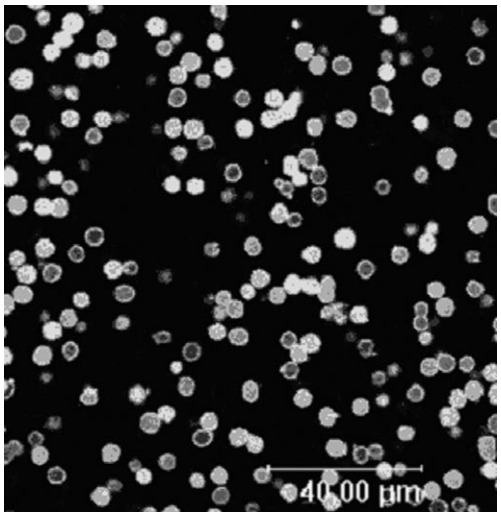

Figure 3. Confocal microscopy image of polyallylamine/polystyrene sulfonate polyelectrolyte capsules loaded with fluorescein-labeled bovine serum albumin.

Usually, the polyelectrolyte capsule shell is permeable for macromolecules and nanoparticles at low pH (<3) or high ionic strength while it is in a "closed" state at neutral pH. A possible explanation of the permeability properties of the polyelectrolyte shell can be provided by considering the polyelectrolyte interactions in the shell wall. Under the conditions of capsule formation (pH 7), the charge densities on both polyelectrolytes determine their stoichiometric ratio during adsorption. Since the polymers are irreversibly adsorbed in the shell wall, a pH decrease does not induce polymer desorption. However, charging of one of the polyelectrolytes may occur, which would induce positive (negative) charge into the shell wall. This may alter the shell-wall morphology by enhancing the repulsion, which could lead to defects in the polyelectrolyte shell.

The possibility of switching the capsule shell between an open and closed state provides an efficient tool for the uptake and release of the active materials. For instance, the capsules can be loaded at low pH and after increasing the pH the material is captured inside. The possibility of controlling the loading and release of macromolecules into and out of polyelectrolyte capsules may find widespread application in self-repairing coatings.[34] Organic solvents can also induce permeation through the LbL-assembled shell. Using a 1:1 ethanol/water mixture, Lvov et al.[35] encapsulated urease (5-nm-diameter globules) in poly(allylamine)/poly(styrene sulfonate) capsules. Ethanol might partially remove the hydration water between the polyelectrolytes, leading to a segregation of the polyion network and the formation of pores.

Polyelectrolyte capsules composed of poly(allylamine)/poly(styrene sulfonate) multilayers preserve their integrity after heating at 120 °C for 20 min in aqueous solution but show a considerable decrease in size (50–70 % depending on the diameter of the initial capsules, Figure 4).[36] The diameter decrease is accompanied by a strong increase of layer thickness and decrease of permeability, which leads to en-

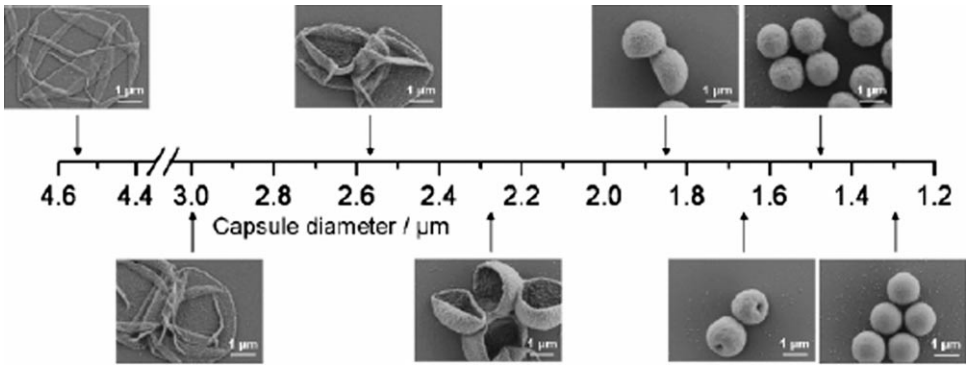

Figure 4. Scanning electron microscopy (SEM) images of polyelectrolyte capsules shrunk to different sizes as a function of diameter after temperature treatment (reprinted from Ref. [36]. Copyright, American Chemical Society).

hanced entrapment capabilities. The capsules become impermeable even for low-molecular-weight compounds. The driving force for this polyelectrolyte rearrangement process is the entropy gain through the more coiled state of the polyions and the decreased interface between polyelectrolytes and water. Probably some water, which fills the pores of the multilayers, is expelled during the high-temperature treatment.

Water-soluble polyelectrolyte nanocapsules can be synthesized by vesicular or emulsion polymerization via core/shell latexes. These capsules, formed by a covalently crosslinked poly(acrylic acid) shell, show a reversible pH- and ionic-strength-dependent swelling transition causing a considerable increase (decrease) of their radius.[37] The carboxylate groups of nanocapsules dissociate increasingly with increasing pH. As a result of the associated electrostatic repulsion between the increasing number of the identically charged carboxylate anions, the shells of such particles swell considerably upon raising the pH value. The radius of crosslinked poly(acrylic acid) capsules increases from about 45 nm at $pH < 4$ to about 195 nm for $pH > 9$. This swelling is completely reversible. Poly(acrylic acid) capsules precipitate at $pH < 3.5$, which provides a convenient route to isolate and purify the loaded capsules.

2.3. Sonoinduced Fabrication of the Nanocontainers

Another approach to fabricate nanocontainers is to employ a cavitation microbubble as a template on whose surface an organic or inorganic shell is formed from monomers, precursors, and nanoparticles adsorbed at the cavitation interface. Ultrasound has frequencies from 20 kHz to 1 GHz. Ultrasonic energy is concentrated through acoustic cavitation.[38] Bubble collapse in liquids results in an enormous concentration of energy from the conversion of the surface energy and kinetic energy of the liquid motion into heat or chemical energy. The high local temperatures (5000–7000 K inside the microbubble) and pressures combined with rapid cooling provide unique conditions for forming micro- and nanocontainers.[39]

High-intensity ultrasound (3 min at an acoustic power of $\approx 150\ W\,cm^{-2}$) applied to bovine serum albumin, human serum albumin, and bovine hemoglobin protein solutions results in both air-filled microbubbles and nonaqueous liquid-filled protein microcapsules.[40] These microcontainers are stable for months. The mechanism responsible for the formation is a combination of two acoustic phenomena: emulsification and cavitation. The shell of protein containers is primarily formed by disulfide crosslinking of cysteine residues between protein molecules. The primary oxidizing agents are superoxide ions (HO_2), which are generated from water and oxygen during acoustic cavitation. The crosslinked shell of the microcontainers is about six protein molecules in thickness.

The characteristics of the ultrasonically obtained containers can be changed to increase their stability and loading capacity. This can be done by decorating the surface of the nanocontainers with suitable hydrophilic and hydrophobic moieties functioning as selective ligands (such as L-cysteine, L-lysine, poly(L-lysine), chitosan, and β-cyclodextrin).[41] Additional stability and functionality was achieved employing the layer-by-layer deposition approach.[42] Electrostatic layer-by-layer assembly of polyelectrolyte multilayers (polyallylamine, poly(styrene sulfonate)) was successfully accomplished on the surface of a capsule made by ultrasonic agitation of a mixture of Span/Tween block co-polymers. The resulting polyelectrolyte shell stabilizes the overall containers against collapse for at least a week. The stability of the capsules gradually increases with the number of deposited polyelectrolyte layers, however, at eight or more polyelectrolyte layers the additional stabilization effect of the next layer decreases, reaching almost zero at 12 layers.

Hollow inorganic spheres can be produced during ultrasonic treatment by either ultrasonically induced reactions between initial precursors (salts) at the gas/liquid interface of the cavitation microbubble or by melting and condensation of the surface-modified nanoparticles at this interface. PbS hollow nanospheres with diameters of 80–250 nm have been synthesized by a surfactant-assisted sonochemical route from $Pb(CH_3COO)_2$, thioacetamide, and sodium dodecylbenzenesulfonate.[43] Structural characterization indicates that shells of the hollow spheres are composed of 12 nm PbS nanoparticles. Surfactant-assisted ultrasonic synthesis was proved to be effective and appealing because surfactants can act as soft templates as well as structure-direct-

ing agents for the assembly and subsequent mineralization of inorganic precursors at the surfactant–solution interface. Hollow nanospheres such as CdSe and MoS_2 were also prepared by this method.[44]

Submicrometer hollow silica spheres with mesoporous walls were prepared by the application of ultrasound to a mixture of nonionic polyoxyethylene surfactant and tetraethylorthosilicate, which gave a stable emulsion with the cavitation bubbles created by the ultrasound trapped inside.[45] The silica prepared with a sonication power of 120 W is made of 200–400 nm hollow spheres with mesoporous walls. The final structure of the resulting silica particles depends on the hydrophilic and hydrophobic components. SiO_2 microcontainers were obtained by ultrasonic treatment (20 kHz) of SiO_2 nanoparticles in the presence of cetyltrimethylammonium bromide (CTAB) and $NaHCO_3$.[12] Optimal SiO_2 and cetyltrimethylammonium bromide concentrations are 1 wt.% and 0.5 mM, respectively. The quantity of the resulting SiO_2 containers increases with the increase of ultrasonic power (up to 500 W). The resulting SiO_2 containers have micrometer-scale size (Figure 5) and are mechanically stable. During ultrasonic treatment of the CTAB/SiO_2 aqueous sol in the presence of $NaHCO_3$, initial gaseous nucleation centers rapidly expand forming micrometer-sized cavitation microbubbles. CTAB molecules on the silica surface render the silica nanoparticles more hydrophobic, which promotes their anchoring at the gas/liquid interface forming a preliminary silica shell around the gaseous nucleation core. This shell becomes more dense during the following microbubble expansion capturing additional SiO_2 nanoparticles from the adjacent bulk solution. Specific conditions at the cavitation interface result in partial crystallization of the amorphous silica nanoparticles producing a quartz phase and a high degree of interconnection between the silica nanoparticles in the microsphere shell.

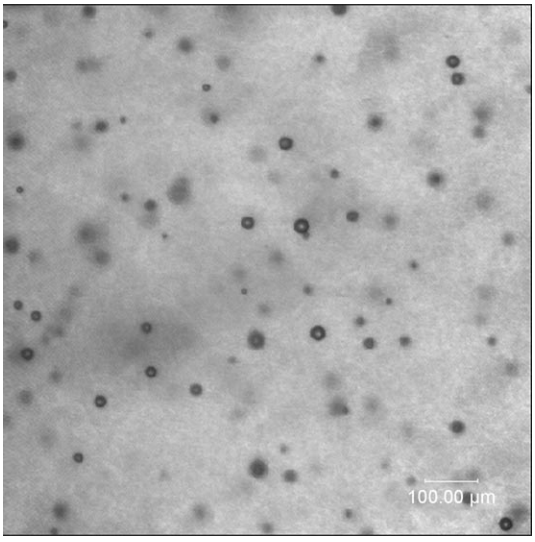

Figure 5. Confocal microscopy image of silica microspheres taken in bright-field mode.

3. Self-Healing Surfaces

3.1. Self-Repairing Polymeric Materials

There are several types of coatings and self-healing or self-repairing mechanisms. The first one and the oldest one was employed for auto-repairing polymers and polymer coatings. The main idea was to introduce micrometer-scale containers into the polymer body. These containers were filled with monomers similar to the nature of the polymer matrix and an appropriate catalyst or UV-sensitive agent to initiate the polymerization of the monomer released at the damaged place of the polymer coating. Mechanical deformation of the microcontainers was employed for starting the release of the monomer and repairing (sealing) of the defects. The technique focused on the cracking of hollow repair fibers dispersed in a matrix and the subsequent timed release of repair chemicals, which result in the sealing of matrix cracks, the restoration of strength in damaged areas, and the ability to retard crack propagation.[46] A propagating crack ruptures the microcapsules and exposes catalyst particles. Crack opening draws the healing agent into the defect area, where contact with the catalyst phase initiates polymerization. The polymerized healing agent reestablishes structural integrity across the crack plane. Several investigations of microcontainer-incorporated polymers have appeared in the literature using microballoons, hollow particles, hollow microspheres, and bubbles.[47]

Materials capable of smart self-repair consist of several parts: a stimulus to release the repairing chemical such as the cracking of a microcontainer; a microcontainer; a repair chemical monomer carried within; and a method of hardening the microcontainer load in the polymer matrix. Typical macroscopic damage involves destruction of a material due to impact. On the microscale, damage such as matrix microcracking alters mechanical properties such as strength, stiffness, and dimensional stability depending on the material type. Thermal, electrical, and acoustical properties are changed as the matrix cracks. Microdefects act as sites for environmental degradation, as well as for nucleation of the macrodefects. The repair of microdamage can be accomplished by incorporating an appropriate number of time-release repair containers into a container-reinforced polymer matrix composite. The samples in which prior release of a crosslinking adhesive into a cracked matrix is allowed to set up over a time have greater strength and ability to repair than the specimens that had no crosslinking adhesive internally released.[48] The internal delayed release of adhesive improves impact strength and the ability to deflect while carrying a load.

Microencapsulated dicyclopentadiene (DCPD) healing agent and highly porous Ru catalyst were incorporated into an epoxy matrix to produce a polymer composite capable of self-healing (Figure 6).[46] Both the virgin and healed fracture toughness depend strongly on the size and concentration of the microcapsules added to the epoxy. Addition of dicyclopentadiene-filled urea formaldehyde microcapsules into epoxy samples yields up to a 127% increase in coating toughness. The increased toughening associated with fluid-

small NANO MICRO

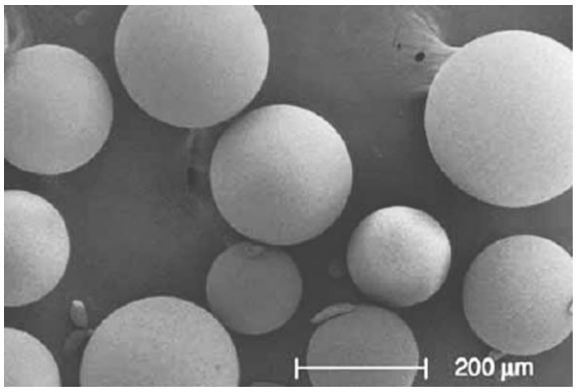

Figure 6. Urea formaldehyde microcapsules containing dicyclopentadiene (reprinted from Ref. [46]. Copyright, Kluwer Academic Publishers).

filled microcapsules is attributed to the healing of subsurface microcracking. Overall the embedded microcapsules provide two independent effects: the increase in virgin fracture toughness from general toughening and the ability to self-heal the virgin fracture event. Healed fracture toughness increases steadily with microcapsule concentration until reaching a plateau at about 20 vol%. The maximum healing efficiency for 180 μm microcapsules occurs at low concentrations (5 vol%). For 50 μm microcapsules, high healing efficiency only occurs at higher microcapsule concentrations (20 vol%) since more capsules are required to deliver the same volume of DCPD healing agent to the fracture plane.

Diene monomers (DCPD and 5-ethylidene-2-norbornene) and their blends were investigated as candidate self-healing agents with a Grubbs catalyst.[49] It was found that the reaction becomes faster with increasing 5-ethylidene-2-norbornene content at lower catalyst loading. Rigidity after curing for 120 min was the highest in a 1:3 DCPD/5-ethylidene-2-norbornene blend when it was cured on the epoxy resin coating. Considering requirements for effective self-healing (i.e., fast reaction during cure, high rigidity after cure, reduction of catalyst amount, and lower temperature capabilities), DCPD/5-ethylidene-2-norbornene blends are very good candidates for self-healing agents. The inherent shortcomings of the method based on diene monomers are the potential side reactions with the polymer matrix and air. These reactions could be avoided by using tin-catalyzed polycondensation of phase-separated droplets containing hydroxy end-functionalized polydimethylsiloxane and polydiethoxysiloxane.[50] The catalyst, di-*n*-butyltin dilaurate, is contained within polyurethane microcapsules embedded in a vinyl ester matrix and is released when the capsules are broken by mechanical damage. The healing chemistry of this system remains stable in wet environments and at an elevated temperature (>100 °C). No reactions take place between the loaded components prior to exposure to the catalyst. When the matrix cracks, a mixture of catalyst released from microcapsules and the healing agent wets the entire crack plane. Addition of an adhesion promoter to the matrix optimizes wetting and bonding of the crack faces.

Repair of macroscopic adhesion defects formed throughout the service life of the composites was carried out involving the filling of hollow fibers with a polymer resin, which then fracture under excessive loading of the structure.[51] The secondary system was added to the hollow fibers, which are capable of migrating to and repairing the defect, providing improved adhesion and durability (Figure 7). Secondary components could be methyl methacrylate, 2-ethylhexylmethacrylate, *t*-butylamino ethyl methacrylate and lauryl methacrylate for fixing adhesion of the polypropylene matrix. CdSe/ZnS nanoparticles dispersed in a polymer poly(methylmethacrylate) matrix were found to migrate to a crack generated at the interface between the polymer and a glassy layer.[52] Segregation of the nanoparticles to the crack depends on both the enthalpic and entropic interactions between the polymer and nanoparticles. In particular, poly(ethylene oxide)-covered 5.2 nm spherical nanoparticles in a poly(methyl methacrylate) matrix diffused to cracks in the adjoining silicon oxide layer, whereas tri-*n*-octylphosphine oxide-covered nanoparticles did not. These results point to a simple means of fabricating systems that can self-heal the substrate/coating interface improving the durability of multilayered systems.

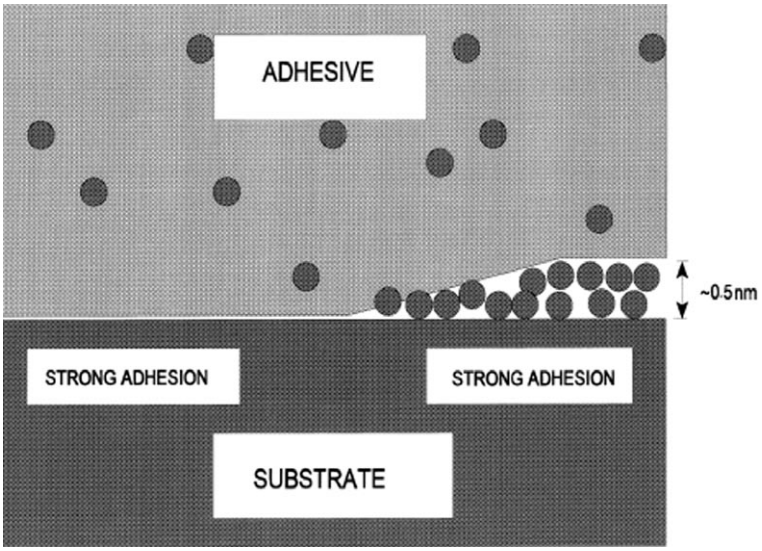

Figure 7. Adhesive joint after migration of impregnated active agents (reprinted from Ref. [51]. Copyright, Elsevier Science B.V.).

Polyelectrolyte-based aqueous poly(L-lysine)-*graft*-poly(ethylene glycol) (PLL-*g*-PEG) was employed as a self-healing agent in an oxide-based tribosystem.[53] Rapid self-healing of PLL-*g*-PEG is attributed to electrostatic interactions between the polycationic poly(L-lysine) backbone of the polymer and the negatively charged oxide surface. The polycationic PLL backbone is rapidly attracted to the negatively charged SiO_x surface in aqueous solution at neutral pH. In contrast, a similar healing effect was not readily achievable in the case of methoxy-poly(ethylene glycol) trimethylsilyl-ether (Sil-PEG), a copolymer that is covalently bound to the surface prior to the tribological stress. The mechanism of boundary lubrication is based upon the modification of shear strength of the tribological interface, rather than upon the formation of a hydrodynamic film.

Calcium aluminate fillers (<40 μm) containing monocalcium aluminate and calcium bialuminate reactants as the major phases were tested in the biomimetic healing and repairing of micrometer-sized cracks generated in a poly(phenylenesulfide) coating. They were evaluated by exposing the cleaved coatings to a simulated geothermal environment.[54] The decalcification/hydration reactions of the monocalcium aluminate and calcium bialuminate enclosed in the cracks led to rapid growth of boehmite crystals, while the crystalline calcite phase formed by the carbonation of these reactants was leached out of cracks because of the formation of water-soluble calcium bicarbonate. During exposure for 24 h, the blocklike boehmite crystals (≈ 4 μm in size) densely filled and sealed the open cracks. Extending the exposure time to 20 days resulted in no change in pore resistance, suggesting that the sealing of the cracks by boehmite crystals played an essential role in reconstituting and restoring the function of the failed coatings as a corrosion-preventing barrier. Therefore, poly(phenylenesulfide) coatings filled with fillers are able to self-heal cracks. The demonstrated biomimetic approach provides an effective way to recover mechanical strength and highlight concealed damage after an impact event. A significant fraction of lost flexural strength can be restored by the self-repairing effect of a repair agent stored within the fibers. A natural self-reinforced composite material, bamboo, was studied as a self-repairing biomedical material.[55] Its anatomical structure was investigated and compared with those of some common bone-bonding or bone-repairing biomaterials. Bamboo has the closest modulus of elasticity to the human thighbone. After grafting a polymer whose monomer includes poly(ethylene glycol) and di(aminopropyl)poly(ethylene glycol) on bamboo, the bamboo has the ability to form a calcium phosphate coating after being immersed in a calcification solution (simulated body fluid and accelerated calcification solution).

Micellar coatings of surfactants at solid–liquid interfaces can provide colloidal stability, corrosion inhibition, and boundary lubrication. Highly ordered, self-assembled micellar structures formed by surfactants at the solid–liquid interface were revealed.[56] Depending on the surfactant/surface combination, different morphologies such as full- or half-spherical and cylindrical micelles were found. On surfaces, the previously measured diffusion constants of 10^{-12} to $10^{-10}\,m^2 s^{-1}$ would allow the closing of a 20-nm-diameter hole within a few microseconds. The reorganization process described here is mainly because of redistribution of surfactant molecules on the surface rather than the exchange of the surfactants between the bulk liquid and the surface. Nanometer-scale defects in an array of surfactant surface micelles are cured within 6 ms.

With very recent developments in nanotechnology, elaborate and multifunctional surface coatings with precise architectural and chemical control on the nanoscale are becoming easily accessible. Layer-by-layer deposition techniques, nanoparticle surface-modification chemistry, and nanoreactor chemistry were employed to construct thin-film coatings with two distinct layered functional regions: a reservoir for the loading and release of bactericidal chemicals and a nanoparticle surface cap with immobilized bactericides.[57] A reservoir region made of 20 bilayers of poly(allylamine hydrochloride) (assembly pH 8.5) and poly(acrylic acid) (assembly pH 3.5) and a cap region made of 10 bilayers of poly(allylamine hydrochloride) (assembly pH 7.5) and silica nanoparticles (20 nm in diameter, assembly pH 9.5) were constructed successfully through polyelectrolyte LbL deposition followed by Ag-nanoparticle formation inside polyelectrolyte multilayers (Figure 8). Dual-functional coatings showed very high initial bacteria-killing efficiency due to the release of Ag ions and retained significant antibacterial activity after the depletion of embedded Ag because of

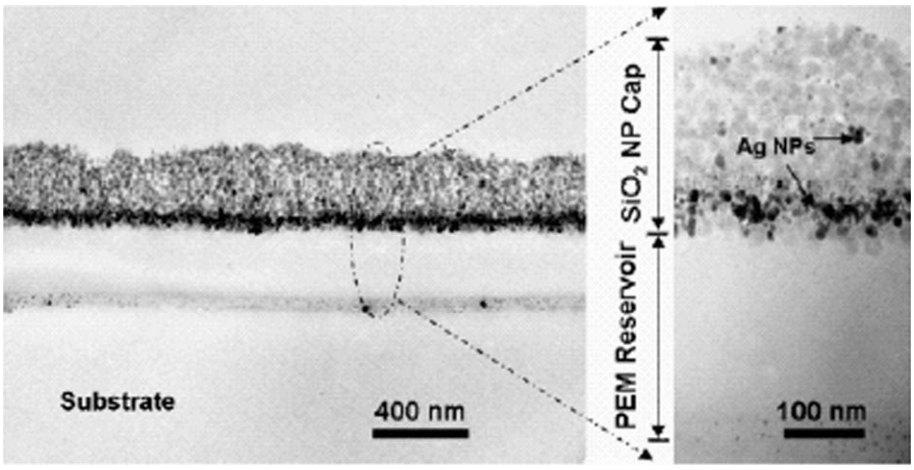

Figure 8. Cross-sectional TEM images showing two-level antibacterial coatings. Ag nanoparticles resulting from two Ag loading and reduction cycles were embedded inside the coatings by using a wet-phase-reduction method using a dimethylamine–borane complex solution (reprinted from Ref. [57]. Copyright, American Chemical Society).

the immobilized quaternary ammonium salts. This coating scheme is not limited only to silver and quaternary ammonium salts but should allow the incorporation of a variety of other antibacterial agents such as antibiotics and titanium dioxide.

A similar layer-by-layer approach was involved in the fabrication of other types of functional coatings with fast feedback response. The superhydrophobic behavior of the lotus leaf structure can be mimicked by creating a honeycomb-like polyelectrolyte multilayer surface overcoated with silica nanoparticles. Superhydrophobicity was achieved by coating this highly textured multilayer surface with a semifluorinated silane.[58] The film was then heated to 650 °C to remove the polyelectrolytes and to create the surface texture needed for superhydrophobic behavior. A self-cleaning and corrosion-resistant surface results since the rolling water droplets remove dirt and debris. Multifunctional nanoporous thin films exhibiting both antifogging and antireflection properties were fabricated from LbL-assembled silica nanoparticles and a polycation.[59] The antifogging properties are a direct result of the development of superhydrophilic wetting characteristics. The nearly instantaneous sheetlike wetting promoted by the superhydrophilic multilayer prevents light-scattering water droplets from forming on a surface. The low refractive index of the multilayer film (as low as 1.22) resulting from the presence of nanopores was found to impart excellent antireflection properties. The assembly conditions (solution pH and nanoparticle concentration) as well as the choice of nanoparticle size were found to strongly influence film properties. Hydrophilic patterns on superhydrophobic surfaces were created from water/2-propanol solutions of a polyelectrolyte to produce surfaces with extreme hydrophobic contrast.[60]

3.2. Self-Healing Coatings for Metal Protection

Nanotechnology applications in the automotive and aerospace industries have become particularly significant over the last decade.[61] Visions of "nano in cars" range from contributions towards CO_2-free engines, safe driving, reduced noise, self-healing bodies and windscreens, "chameleon" colors, and a self-forming car body. For automotive components, nanoparticles, -dots, -pores, -fibers, -tubes, and -layers either dispersed within a matrix material (nanocomposites), or arranged on surfaces (nanostructured surfaces) offer exclusive potential. Volume effects such as diffusion, absorption, and mechanical strength, as well as surface effects such as adsorption, hardness, and self-repairing reactions have been achieved. Self-organization of structures will play an essential role in growth, deposition, and etching.

Nanotechnology is already in mass production. Antireflection coatings based on multiple nanolayers on glass (trade name Schott Conturan) are used by Audi and DaimlerChrysler. Sun-protecting glazing with infrared reflecting nanolayers embedded into glass (trade name Sekurit Thermocontrol) is already used in buses (e.g., Evobus). Thermoplastic nanocomposites with nanoflakes (trade name Basell TPO-Nano) are applied for light exterior vehicle parts by General Motors. "Chameleon" coatings were prepared using nanocomposite structures consisting of crystalline carbides, diamond-like carbon, and transition-metal dichalcogenides.[62] Various mechanisms were found to achieve coatings that exhibited surface self-adaptation and supertough characteristics, including the transition of mechanical response from hard and rigid to quasi-plastic by grain-boundary sliding at loads above the elastic limit, friction-induced sp^3/sp^2 phase transition of the diamond-like carbon phase, and recrystallization and reorientation of the dichalcogenide phase.

The corrosion resistance of stainless steel is attributed to the formation of a passive film, which protects the material from continuous corrosion attack. However, when subjected to an attack combining corrosion and erosion, the passive film can be damaged by solid-particle impingement resulting in exposure of a bare metal surface to the corrosive medium and thus increasing the corrosion/erosion rate. Approaches for resisting the synergistic attack of erosion and corrosion include alloying elements and surface modification to achieve self-healing characteristics.[63] It was demonstrated that yttrium can improve the resistance of stainless steel to sliding wear in corrosive environment. Yttrium renders the anodic protective coating more inert to electrochemical attack and activates the self-healing ability of the anodic coating. In natural environments, unsealed or poorly sealed anodized films are subjected to two opposing effects because of their absorbing properties: self-sealing, which results in gradual protection of the metal substrate; and deterioration. Depending on the particular environment, one phenomenon prevails over the other. Electrochemical impedance spectroscopy studies revealed a self-sealing process for an unsealed anodic film in neutral NaCl and Na_2SO_4 solutions.[64] The resistance of the porous layer and the capacitance of the barrier layer increase and the capacitance of the porous layer decreases with immersion time at the initial stage. However, the improving effect of the self-sealing process on film resistance is decreased with the increase of chloride concentration of the solution. The self-repair of an ordered pattern of nanometer dimensions based on the self-compensation properties of anodic porous alumina has been described.[65] In a pretextured pattern formed on Al using an nanoindentation process with an array of convexes, the deficiency sites of the pattern are compensated automatically during the anodization. It was confirmed that deficiencies in the starting Al_2O_3 pattern could be repaired automatically using the self-compensating anodic process. The concept of self-repair of defects in porous alumina coatings resembles the repairing of defects in the bases of DNA strands through a retrial process. The compensated pores are indicated as arrows in Figure 9. It should be noted that the compensated pores were precisely positioned at the center of the six nearest surrounding pores, and that the perfect hexagonal arrangement of the pores was recovered. When the number of deficiencies in the concaves is increased, the accuracy in determining the position of the compensation was decreased, particularly in the case of chained deficiencies.

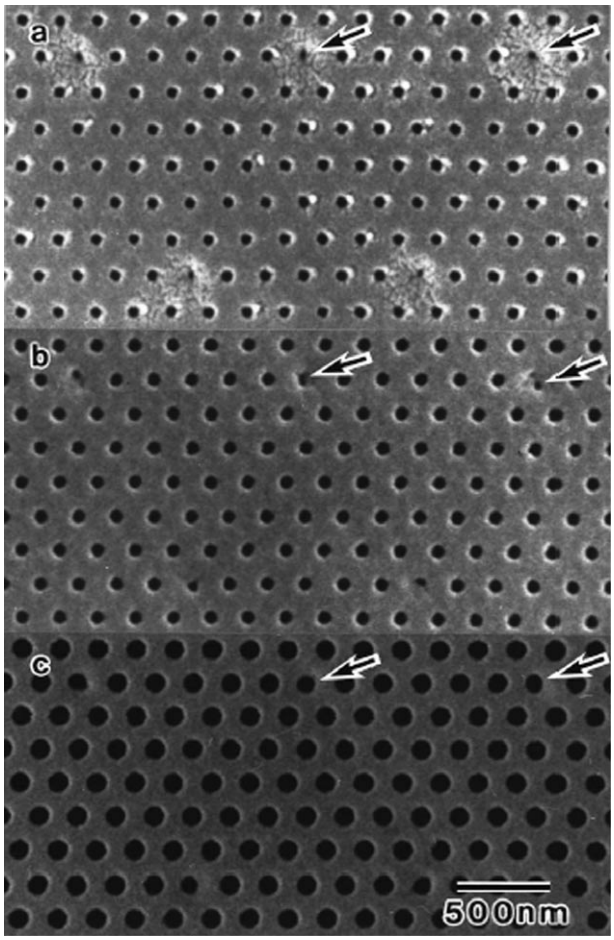

Figure 9. SEM micrographs of anodic porous alumina: As-anodized porous alumina (a), alumina after pore-widening treatment for 20 min (b) and 60 min (c). The anodization of Al was conducted under a constant voltage of 80 V in a 0.5 wt% oxalic acid solution at 17 °C (reprinted from Ref. [65]. Copyright, American Institute of Physics).

A new organic composite coating for enhancing the corrosion resistance of 55% Al–Zn alloy-coated steel sheets has been developed.[66] The new coating is composed of an insoluble chromic compound, phosphate, organic resin, and specially developed corrosion-preventive additives (Cr acid salt, Ca or Mg phosphoric acid salt, and basic oxide), which effect a self-healing action in cracks generated on the surface of the steel sheet while forming. All the coatings showed high insolubility. The coating including a Ca phosphoric acid salt had the highest corrosion resistance of all the tested additives. The oxidation of Cu, Zr, and alloys forming chromia, alumina, and zirconia was studied in a closed reaction chamber in O_2 gas at a pressure of $\approx$20 mbar in order to investigate the self-healing effect of these oxides.[67] The experimental results indicated that hydrogen in the metal substrates induces increased metal-ion transport in internal oxide surfaces during oxidation, which leads to increased oxide growth at the oxide–gas interface. A balanced transport of metal and oxygen ions in metal oxides, which leads to oxide growth at both the metal–oxide and oxide–gas interfaces, is found to be favorable for the formation of protective oxides with good adherence to the metal substrate. Depending on the original proportion of metal-to-oxygen ion transport in the oxide, an addition of hydrogen will increase or decrease the oxidation kinetics. Simultaneous metal-cation and oxygen-anion transport is a prerequisite for the formation of protective metal oxides with low densities of pores, cavities, and cracks.

Electrochemical impedance spectroscopy was used to study the film formation, destruction, and corrosion protection mechanism of a carbon dioxide (CO_2) corrosion inhibitor, imidazoline,[68] which is most commonly used for protecting oil wells, gas wells, and pipelines from CO_2 corrosion. Imidazoline is a very effective CO_2 corrosion inhibitor, which forms a chemically bonded film on the metal surface inside the pipeline. The inhibitor film seems to have a multilayered structure, which is a combination of an inner layer and many outer layers of inhibitor molecules with possible inhibitor molecular crosslinking. The multilayer characteristic of the inhibitor film showed strong self-repairing ability and good persistency under the testing conditions, although surface shear stress gradually removed the inhibitor film and caused inhibitor film failure. As the inhibitor film is broken down locally, the corrosion rate increases greatly in these small areas and outer layers of the imidazoline migrate to the local damaged area blocking the corrosion process.

Another interesting approach to achieve self-healing in anticorrosion coatings is to employ conductive polymers (polypyrrole, polyaniline, polythiophene) as a coating component. Polypyrrole doped with $[PMo_{12}O_{40}]^{3-}$ polyanions revealed significant self-healing in corrosion protection.[69] Responsive release of the inhibitor ($[PMo_{12}O_{40}]^{3-}$) occurs only when the potential at the interface decreases at an active defect. However, the release mechanism can be negatively affected by the presence of small cations. Hence, such a self-healing coating has to be carefully designed in order to ensure effective performance. A possible mechanism for the case of polyaniline was also described by Kendig et al.[70] Such a coating releases anions only in the case of corrosive attack and prevents them from being leached out or being released by ion-exchange processes. Even large defects can be passivated because the switch for anion release decreases the potential at the metal/polymer interface during the delamination. A significant inhibition of the delamination is provided on demand by polyanion release. The release of $[PMo_{12}O_{40}]^{3-}$ ions is truly electrochemical and not influenced by pH at the metal/polymer interface. A conductive polymer release system, which is unaffected by leaching and pH changes and safely stores the corrosion inhibitor ions (as counterions for the polymer chain) can be used as an intelligent corrosion-protecting coating.

3.3. Ce-Based Self-Healing Pretreatments

The development of new effective anticorrosion pretreatments for metallic substrates is an issue of prime importance for corrosion science due to the fact that chromates must be banned for environmental reasons. Removal of hex-

NANO MICRO small

avalent chromium from the industry opens a significant gap in the corrosion-protection technologies. One of the possible replacements of the chromates is hydrated cerium(III) oxide, Ce_2O_3. A self-healing protective film was prepared on a zinc electrode by treatment in 10^{-3} M $Ce(NO_3)_3$ at 30 °C for 30 min to form a thin layer of hydrated Ce_2O_3.[71] The protection efficiency of the cerium film was 97.7% after an immersion time of 24 h and 95.6% at 240 h. Neither a pitlike anodic dissolution feature (PLF) nor a pit was observed within the scratches after 72 h of incubation in 0.5 M NaCl solution. X-ray photoelectron spectroscopy and electron-probe microanalysis revealed that Ce^{3+} ions migrate into the scratches to form a new layer of hydrated Ce_2O_3 within the scratches resulting in the self-healing activity of the film. Hence, pitting corrosion at the scratched surface was fairly prevented during immersion in the solution for many hours.

It is considered that a layer consisting of hydrated or hydroxylated Ce_2O_3 formed on the surface of zinc oxide or hydroxide [ZnO]OH by direct adsorption of partially hydrated or hydroxylated Ce^{3+} ions, for example:

$$[ZnO]OH + Ce^{III}OH \rightarrow [ZnO]OCe^{III}OH + H^+$$

The hydrated or hydroxylated Ce^{3+} ions react repeatedly at the defect site:

$$[ZnO]OCe^{III}OH + Ce^{III}OH \rightarrow [ZnO]OCe^{III}OCe^{III}OH + H^+$$

$$2\,[ZnO]OCe^{III}OH \rightarrow [ZnO]OCe^{III}(OH)OCe^{III}O[ZnO] + H^+$$

$$[ZnO]OCe^{III}(OH)OCe^{III}O[ZnO] + Ce^{III}OH \rightarrow [ZnO]OCe^{III}(OCe^{III}OH)OCe^{III}O[ZnO] + H^+$$

constructing a dense Ce(III) oxide layer on the substrate surface, terminating the corrosion.

A self-assembled monolayer of the hexadecanoate ion $C_{15}H_{31}CO_2^-$ was prepared on a zinc electrode coated with a layer of hydrated cerium(III) oxide.[72] A more positive open-circuit potential of the coated electrode was maintained during immersion in the solution for 4 h compared to that of an uncoated one, and polarization curves showed marked suppression of the anodic process. The protection efficiency of the hybrid coating is more than 99%. A stable adsorption bond was formed between Ce^{3+} and $C_{15}H_{31}CO_2^-$ ions resulting in an ordered and close-packed arrangement of the $C_{15}H_{31}CO_2^-$ monolayers on the formed Ce_2O_3 surface. The migration of $C_{15}H_{31}CO_2^-$ ions adsorbed on the surface of a Ce_2O_3 layer containing Zn^{2+} ions caused repassivation at a defect of the layer resulting in maintenance of the passive film against breakdown and a high degree of protection against corrosion of zinc in 0.5 M NaCl.

A highly self-healing, protective film against corrosion of zinc in aerated 0.5 M NaCl was prepared by coating the electrode surface with a Ce_2O_3/Na_3PO_4 composite from 10^{-3} M $Ce(NO_3)_3$ + $Na_3PO_4{\cdot}12H_2O$ at 30 °C for 30 min followed by drying at 30 °C for 23 h.[73] Neither a PLF nor a pit was formed on the scratched surface even after 120 h in 0.5 M NaCl and only a PLF appeared at the scratches after 360 h. The film was composed of an outer layer of Na_3PO_4, an intermediate layer of $Zn_3(PO_4)_2$, and an inner layer of Ce_2O_3. Addition of the $Ca(NO_3)_2$ or $Mg(NO_3)_2$ to the $Ce_2O_3 + Na_3PO_4$ film resulted in increased protection ability but less pronounced self-healing effects. Cerium sulfate was used as the main composite in solution to prepare a yellow chemical conversion film on magnesium alloy.[73c] The results showed that when there is no other component in the solution besides cerium sulfate, a yellow film can be obtained on the magnesium alloy, but it is not stable. The stability of the cerium protection film increases with added hydrogen peroxide and Al^{3+} ions as were tested in a 3.5% NaCl solution.

3.4. Hybrid Sol–Gel Coatings

Sol–gel films have great potential as coatings (pretreatments) for metal protection. Inorganic sol–gel derived films offer good adhesion between metals and organic paint. However, they have high crack-forming potential. Introduction of an organic component to an inorganic sol–gel system leads to the formation of thicker, more flexible and functionalized films with enhanced compatibility to additional organic top coatings.[74] In this hybrid coating process, organosilicate nanoparticles with peripheral epoxy functional groups are preformed in an aqueous sol–gel process by hydrolysis and condensation of appropriate organosilanes and are then assembled and crosslinked upon application to the substrate surface.[73b] Chemical structure and organic functionality of the silanes and crosslinking agents can be varied and optimized to achieve the maximum effect on stability of the metal/coating interface. The corrosion-protection performance of the hybrid coatings is only maintained if the coating is undamaged. To improve the corrosion-protection properties of the coating when it is mechanically damaged, the incorporation of potent corrosion inhibitors into the coating is needed. Once trapped within the coating material, the corrosion inhibitor becomes active in the corrosive environment, when the entrapped inhibitor can slowly diffuse out of the host material. Despite the simplicity of this doping method, it is difficult to control leaching of the entrapped inhibitors out of the coating film. Solubility of the inhibitor in the coating solution can also be a concern.

Phosphates, vanadates, borates, cerium, and molybdenum compounds were found to have an inhibiting action on the corrosion processes of different metallic substrates. Voevodin et al. investigated the corrosion-protection properties of epoxy/zirconia sol–gel coatings with incorporated non-chromate inhibitors of $Ce(NO_3)_3$, $NaVO_3$, and Na_2MoO_4.[75] Sol–gel films with $NaVO_3$ and Na_2MoO_4 did not provide adequate corrosion protection due to decrease of the sol–gel network stability. However, the sol–gel coatings with cerium dopants perform at least as well as the undoped epoxy/zirconia films. The critical concentration of the cerium inhibitor is in the 0.2–0.6 wt% range. Higher con-

centrations could lead to the formation of defects in the network of the sol–gel film. An additional inhibition effect was revealed when phenylphosphonic acid was introduced into a hybrid sol–gel matrix containing phenyl groups. The entrapment of phenylphosphonate into the sol–gel matrix occurs due to phosphate–phosphate (P–P interactions).

To improve the corrosion-protection properties of sol–gel-derived hybrid coatings on an aluminum AA2024 alloy, two organic corrosion inhibitors (mercaptobenzothiazole and mercaptobenzimidazole) have been encapsulated within the coating matrix in either the presence or absence of cyclodextrin.[73b] Superior corrosion-protection properties have been found for formulations that contain β-cyclodextrin and can be explained by the act of slow release of the inhibitor from the cyclodextrin/inhibitor inclusion complexes and by the self-healing of corrosion defects (Figure 10). The inclusion complexes are more easily trapped within the cross-linked coating material, making it more difficult for the inhibitor to leach out. The encapsulation of organic corrosion inhibitors into the coating host material as inclusion complexes with cyclodextrin can be considered as effective delivery systems of organic inhibitors in active corrosion-protection applications. The slow release of organic corrosion inhibitor from the molecular cavity of cyclodextrin ensures the long-term delivery of corrosion inhibitor and thus the healing of a damaged coating.

The incorporation of inorganic nanoparticles can be a way of inserting corrosion inhibitors adsorbed on the surface of the inorganic nanoparticles for attaining controlled self-healing properties. Zheludkevich et al. demonstrated the possibility of using zirconia nanoparticles as a reservoir for the storage and prolonged release of a Ce-based corrosion inhibitor.[76] The nanoparticles not only reinforce the hybrid matrix but also absorb Ce^{3+} ions, releasing them during contact with moisture inside the corrosion pit. The use of ZrO_2 nanoparticles as Ce reservoirs provides long-term corrosion protection of the metallic substrate compared to the case where the Ce inhibitor is added to the sol–gel matrix. Several other attempts were made to obtain "intelligent" active corrosion-protection systems based on an ion-exchange pigment being added to the coating system. Dispersions of silica and bentonite-based Ce^{3+} cation-exchangers in the polymer coatings enabled direct release of the inhibitor into the electrolyte in blisters and significantly retarded coating delamination. The active corrosion-protection effect was also revealed in the case of ion-exchanged hydrocalcite pigments doped with Ce^{4+} ions or organic inhibitors.

Another approach for inhibitor entrapment was presented by Lamaka et al.[77] A TiO_x porous layer obtained by template synthesis was used as a nanostructured reservoir for the organic corrosion inhibitor benzotriazole. This provides active corrosion protection and self-healing ability of the coating system. The nanostructured porous TiO_x container layer was obtained by controllable hydrolysis of tetraisopropyl orthotitanate in the presence of the nonionic block copolymer Pluronic F127, forming a cellular network of ≈30 nm titania nanoparticles (Figure 11). The structured and benzotriazole-loaded titania layer was coated with a

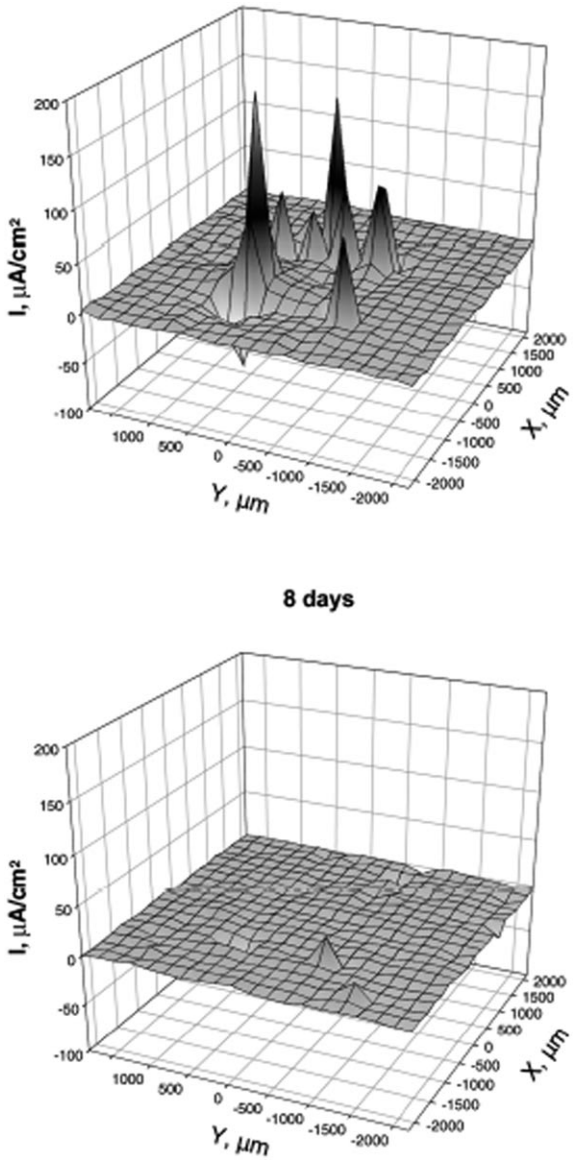

Figure 10. Current-density distribution maps at different immersion times for AlCu artificial defects on AA 2024 alloy coated with nanoparticulate containers. Dopant: mercaptobenzotriazole and β-cyclodextrin at 2.6×10^{-3} M (reprinted from Ref. [74b]. Copyright, Elsevier Science B.V.).

sol–gel-based thin hybrid film (SiO_2/ZrO_2) to provide an additional barrier effect. The pretreatment formed by the nanostructured titania reservoir layer covered with the hybrid film demonstrates well-defined self-healing ability leading to effective long-term active corrosion protection. Only after about 100 h of immersion of the nanocontainer-protected aluminum in 0.05 M NaCl was a slight decrease of the Al_2O_3 underlayer film resistance measured. The first breakdown of the oxide film starts only after 330 h (Figure 12). However the resistance increases again, almost immediately achieving the values before breakdown. Such a breakdown of the oxide layer followed by restoration of the film resistance occurs several times. The nanostructured porous character of the titania layer provides a very high ef-

small NANO MICRO

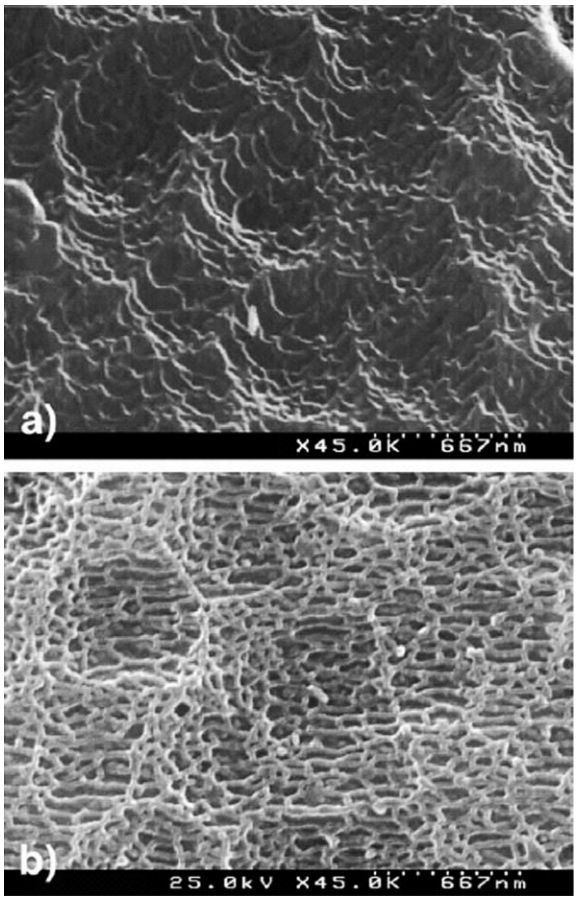

Figure 11. SEM micrographs for AA2024 alloy: a) etched bare substrate, b) etched alloy coated with a nanostructured TiO_x film (reprinted from Ref. [77]. Copyright, Elsevier Science B.V.).

fective surface area for the adsorption of the inhibitor. The developed surface formed by the titania layer also offers good adhesion between the oxide and the sol–gel film due to the high contact area between the two phases.

3.5. Self-Healing Coatings Based on Nanocontainers

Only a few reports on the formation of active surfaces (mostly anticorrosion) based on the release of active material from incorporated nanocontainers are known. Direct deposition of polyaniline-coated polystyrene latex particles (1.85 μm) on an iron plate increased the anticorrosion protection of the iron.[78] Polystyrene latex acts as a carrier for the active polyaniline component. The conducting emeraldine salt form of polyaniline shifted the corrosion potential of the underlying iron into the passive region. Another example of container-based active coatings directly fabricated on a metal surface are heat-expandable spheres for car protection based on ethylvinylacetate derivatives.[79] The coating made from the spheres directly deposited on steel combines two functionalities: improved anticorrosion resistance and increased acoustical insulation.

Coating composition providing self-healing was developed using cellular nanocontainers (diatomaceous earth, zeolite, or carbon-based) dispersed in a polymeric matrix material.[80] Nanocontainers were filled with either an organic (amines, ascorbic acid) or inorganic (borates, zirconates) inhibitor. The possible concentration window of the cellular nanocontainers in the polymer matrix was found to be between 20 and 97 wt.%. If the nanocontainers are less than 20 wt.% of the overall composition, anticorrosive effects are not adequately achieved. On the other hand, if the nanocontainers make up more than 97 wt.% of the overall composition, the polymer material will not be able to form

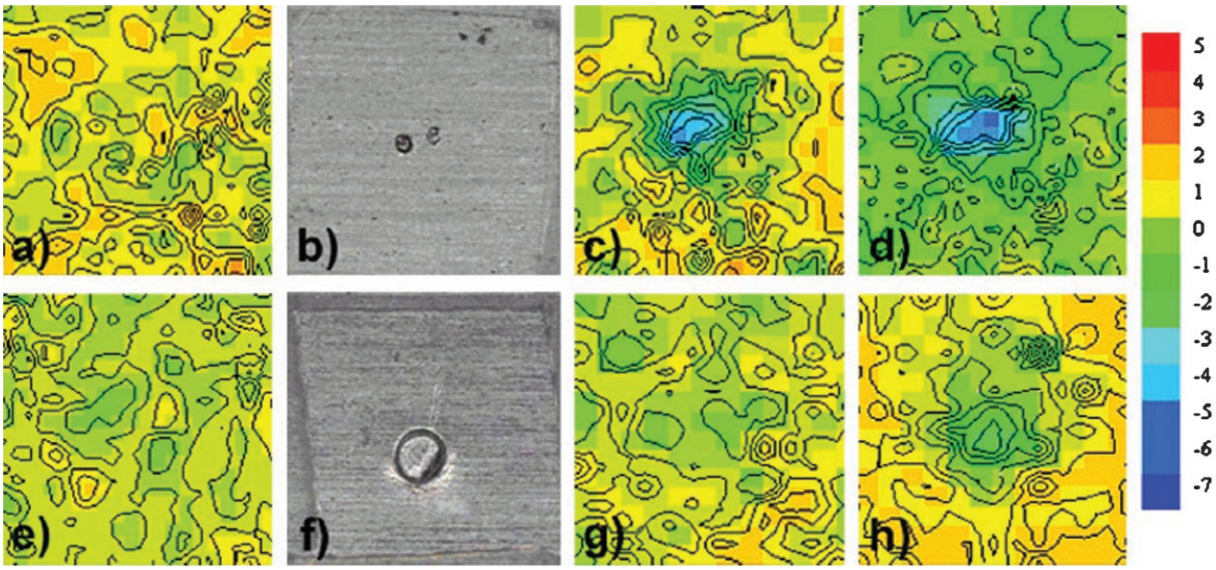

Figure 12. Scanning vibrating electrode maps of the ionic currents measured at 200 μm above the surface of AA2024 aluminum alloy coated with an undoped hybrid film (a, c, d) and with a TiO_x nanostructured coating (e, g, h) exposed to 0.05 M NaCl for 24 h (a, e). Then the defects presented in the microphotographs (b) and (f) were made. Scanning vibrating electrode scans were taken 5 min after defect formation (c, g) and 3 h after defect formation (d, h). Scale units: l A cm^{-2}. Scanned area: 2 × 2 mm (reprinted from Ref. [77]. Copyright, Elsevier Science B.V.).

a continuous matrix and the corrosion would be disadvantageously accelerated.

Chemical binding of the organic inhibitor to aluminum oxyhydroxide nanoparticles was employed to protect aluminum, copper, nickel, brass and bronze.[81] Hydroxide ions generated from the corrosion of these metals trigger the release of bound corrosion inhibitors at $pH > 9$. Here, the release of the inhibitor is maintained only by the corrosion process preventing undesirable leakage. The specific surface area of the aluminum oxyhydroxyde nanocarrier should be at least 100 $m^2 g^{-1}$. Another demonstration of a nanoparticulate inhibitor is an ion-exchange carrier. Compositions include ion-exchange resins, ion-exchanged zeolites, ion-exchanged solid particles, and water-soluble glasses.[82] The corrosion inhibitors are released from the particle surfaces by a subsequent ion exchange with ions (e.g., chlorides, sulfates, sodium ions) transported into the coating via water penetrating through it.

Strong self-healing and long-term active corrosion protection of aluminum was shown by means of the example of benzotriazole-loaded SiO_2 nanocontainers impregnated into a ZrO_x/SiO_x hybrid film.[83] To produce SiO_2 nanocontainers for loading into such a film, the layer-by-layer deposition procedure was employed involving both large polyelectrolyte and small benzotriazole molecules. The suspension of benzotriazole-loaded nanocontainers was mixed following the sol–gel protocol and was deposited onto aluminum alloy by a dip-coating procedure. The uniformly distributed nanoparticles of a diameter about 100 nm were impregnated into the sol–gel film formed on aluminum substrate (Figure 13)

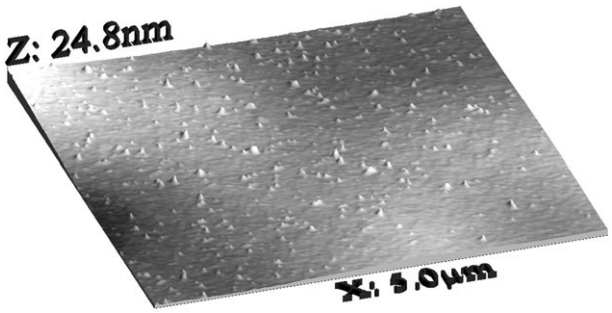

Figure 13. SiO_2/ZrO_2 coatings with benzotriazole-loaded nanocontainers (reprinted from Ref. [83a]).

with an average concentration of the nanocontainers of ≈ 70 per 1 μm^2. AFM does not show any signs of nanocontainer agglomeration.

The release properties and reloading ability of polyelectrolyte-modified halloysite nanotubes, polyelectrolyte-modified SiO_2 nanoparticles, and polyelectrolyte capsules were investigated in order to figure out the most appropriate type of nanocontainers.[83c] The three containers are distinguished by keeping the low-molecular-weight corrosion inhibitor benzotriazole in a hollow lumen inside or within the polyelectrolyte multilayers; SiO_2 nanoparticles coated with polyelectrolyte/inhibitor multilayers; polyelectrolyte capsules with encapsulated inhibitor; polyelectrolyte-coated halloysite kaolin nanotubes, where the depot for inhibitor and release can occur exclusively through the tube opening.

Polyelectrolyte shells, which modified the outer surface of the nanocontainers, were fabricated by the LbL assembly of poly(diallyldimethylammonium chloride)/poly(styrene sulfonate), poly(allylamine hydrochloride)/poly(styrene sulfonate), and poly(allylamine hydrochloride)/poly(methacrylic acid) polyelectrolyte bilayers. The highest reloading efficiency (up to 80%) was observed for halloysite-based nanocontainers, however, after five reloading cycles the efficiency decreased to 20%. For coatings where the immediate release of the inhibitor was necessary, a SiO_2-based or halloysite-based nanocontainer with a shell made of weak polyelectrolytes is preferable. When continuous, gradual release is required, halloysite-based nanocontainers with a shell made of one weak polyelectrolyte and one strong or two strong polyelectrolytes are more favorable.

The nanocontainers exhibit spontaneous release of benzotriazole, the extent depending on the nanocontainer type and the polyelectrolyte shell components (Figure 14a). Despite significant densification of the polyelectrolyte shell after benzotriazole entrapment by the thermal encapsulation method,[36] the capsule is still porous and all of the benzotriazole leaked out after maintaining the capsules for two days in water at pH 6.5. Silica nanoparticles with LbL-assembled polyelectrolyte shells revealed better encapsulation properties. Nanocontainers of this type cannot prevent spontaneous leakage; however, after 60 days of aging the nanoparticulated containers still contain benzotriazole in a quantity up to 80% of the initial benzotriazole loading. Halloysite nanotubes showed the best upkeep characteristics—almost complete suppression of benzotriazole release, with more than 90% of the initial benzotriazole retained inside the inner cavity. This can be explained by the geometrical restriction of the nanotubular container, which is able to release encapsulated material only through polyelectrolyte-blocked edges with diameters of 20–50 nm.

Every corrosion process is accompanied by pH changes in the local corrosion area. The pH value can be reduced or increased depending on the nature of the corrosion process and the metallic substrate and can be used as an effective trigger to open the shell of the nanocontainers, to release the inhibitor into the corrosion pit and, as a consequence, to stop propagation of the corrosion. The pH dependency of the benzotriazole release from halloysite nanocontainers is depicted in Figure 14b. The increase of the release rate both at low and high pH is observed for all polyelectrolyte shells. Poly(diallyldimethylammonium chloride)/poly(styrene sulfonate)-coated halloysite nanocontainers have the slowest release of benzotriazole, and the shell is stable for at least 40 min over the whole pH range. For polyelectrolyte layers containing weak polyelectrolytes, the release rate increases and the shell stability decreases for acidic or alkaline pH regions. This effect is most prominent for halloysites coated with a poly(allylamine hydrochloride)/poly(methacrylic acid)shell. The stability range is narrower for the shell made of weak polyelectrolytes. The poly(allylamine hydrochloride)/poly(styrene sulfonate) shell is stable at $0 < pH < 12$, while the poly(allylamine hydrochloride)/poly(methacrylic

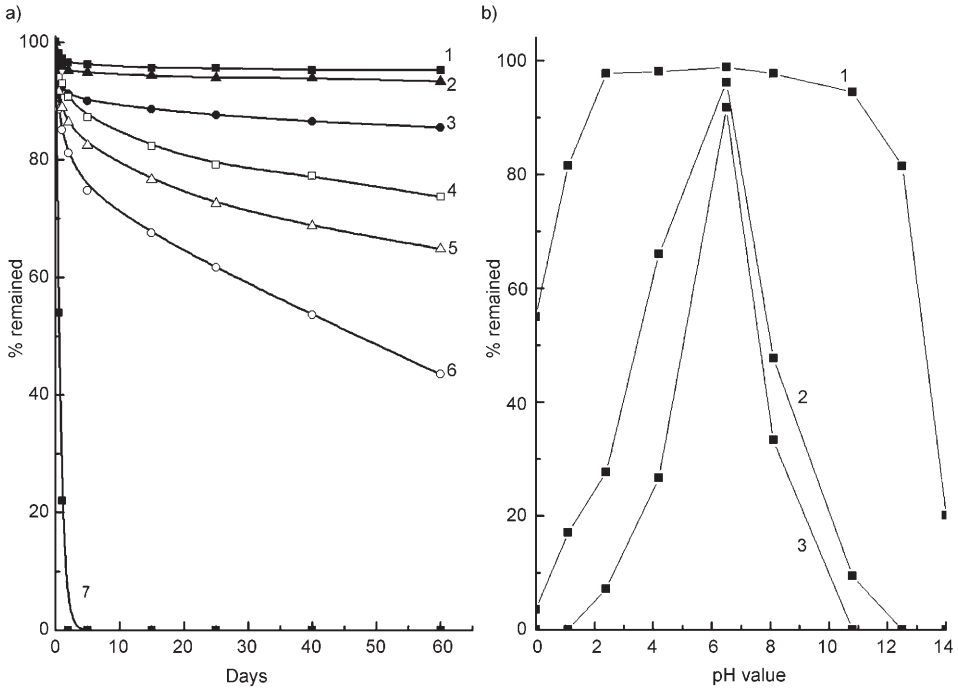

Figure 14. a) Release of benzotriazole during aging of nanocontainers in water at pH 6.5: 1) Halloysite G nanotubes modified with poly(diallyldimethylammonium chloride)/poly(styrene sulfonate) layers, 2) halloysite G nanotubes modified with poly(allylamine hydrochloride)/poly(styrene sulfonate) layers, 3) halloysite G nanotubes modified with poly(allylamine hydrochloride)/poly(methacrylic acid) layers, 4) SiO_2 nanoparticles modified with poly(diallyldimethylammonium chloride)/poly(styrene sulfonate) layers, 5) SiO_2 nanoparticles modified with poly(allylamine hydrochloride)/poly(styrene sulfonate) layers, 6) SiO_2 nanoparticles modified with poly(allylamine hydrochloride)/poly(methacrylic acid) layers, 7) polyelectrolyte capsules made of a poly(diallyldimethylammonium chloride)/poly(styrene sulfonate) shell. b) Release of the benzotriazole release at different pH values (after 30 min of incubation): 1) Halloysite G nanotubes modified with poly(allylamine hydrochloride)/poly(styrene sulfonate layers, 2) halloysite G nanotubes modified with poly(allylamine hydrochloride)/poly(styrene sulfonate) layers, 3) halloysite G nanotubes modified with poly(allylamine hydrochloride)/poly(methacrylic acid)layers.

acid) shell completely dissolves from the halloysite surface at pH values lower than 2 and higher than 10.

Figure 15 shows optical photographs of two aluminum samples; the first was coated by a sol–gel film and the second by a sol–gel film loaded with nanocontainers. Many pit-like defects formed on the surface were found after aging even in a dilute 0.005 M NaCl solution for a pure sol–gel film. The film with nanocontainers does not exhibit any visible signs of corrosion attack even after 14 days in a 100-times more concentrated NaCl solution (0.5 M). This pronounced difference shows the advantages of the "nanocontainer" approach over the direct introduction of inhibitor to the sol–gel coating.[83d]

The self-healing efficiency of the ZrO_x/SiO_x films impregnated with inhibitor-loaded nanocontainers was demonstrated by the scanning vibrating electrode technique. Artificial defects were formed and well-defined cathodic activity appears in place of the induced defect on aluminum coated with an undoped hybrid film. Impressively different behavior was revealed after defect formation on the substrate coated with the ZrO_x/SiO_x film doped with benzotriazole-loaded nanocontainers. No corrosion activity appears in this case after 4 h following the defect formation. Only after about 24 h does a well-defined cathodic activity appear in the zone of the induced defect. However, the defect becomes passivated again two hours later. The most probable mechanism is based on the local change of the pH in the damaged area due to the corrosion processes. When the corrosion processes are started, the pH value is changed in the neighboring area, which opens the polyelectrolyte shell of the nanocontainers in a local area followed by the release of benzotriazole. Then, the released inhibitor suppresses the corrosion activity and the pH value recovers closing the polyelectrolyte shell of the nanocontainers and terminating further release of the inhibitor.

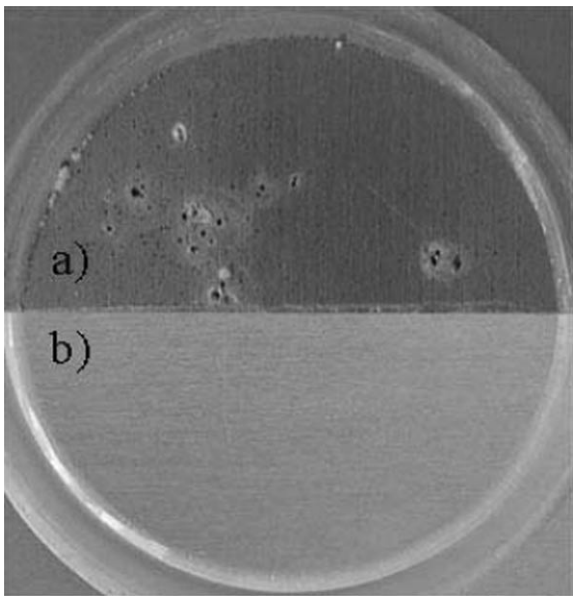

Figure 15. Optical photographs of an aluminum substrate coated with a) a ZrO_x/SiO_x sol–gel film after 14 days in 0.005 M NaCl and b) a ZrO_x/SiO_x sol–gel film impregnated with benzotriazole-loaded SiO_2 nanocontainers after 14 days in 0.5 M NaCl (reprinted from Ref. [83 d]. Copyright, Royal Society of Chemistry).

4. Conclusions and Outlook

Nanocontainers possessing the ability to release encapsulated active materials in a controlled way can be employed to develop a new family of self-repairing coatings. In this Review, several approaches to fabricate self-repairing coatings (sol–gel coatings, Ce-based coatings, self-repairing plastic surfaces, and so on) on plastic and metal substrates were demonstrated. The release of the active materials (e.g., corrosion inhibitors) occurs only when triggered by environmental (corrosion) processes or defects in the coating integrity, which prevents leakage of the active component out of the coating and increases coating durability. The trend for better control of the encapsulation/release parameters is accompanied by progress in the fabrication of the functional nanoreservoirs. Moreover, the active coating can have several active functionalities (e.g., antibacterial, anticorrosion, and antistatic) when several types of nanocontainers loaded with a corresponding active agent are incorporated simultaneously into a coating matrix. This will surely be a matter of future intense research, which, as a result, may lead to highly sophisticated surfaces.

This review also covered some principles and recent developments in the fabrication of nanocontainers with controlled release/uptake properties. The demonstrated universal approach for the fabrication of active coatings is also a great challenge, in order to develop multifunctional organic and composite nanocontainers able to encapsulate active material, retain it in the inner volume for a long period, and immediately release it on demand. Due to their low dimensionality and semipermeable shell, the nanocontainers can be also employed in various areas such as drug-delivery systems, nanoreactors, feedback-active surfaces, and fuel cells. The trend for better control of the encapsulation/release parameters is accompanied by progress in the fabrication of functional nanoreservoirs. In many cases, the detailed mechanisms of the nanocontainer permeability are not yet well understood. This requires additional efforts to investigate kinetic and structural properties of the nanocontainer shell and diffusion of the released active material inside the coating matrix. However, there is no doubt that nanocontainers will create countless new opportunities in research and also in technologies for the fabrication of active composite materials.

Acknowledgements

This work was supported by EU FP6 project "Nanocapsule" (contract no. MIF1-CT-2004-002462) and the NanoFutur program of the German Ministry of Education and Research (BMBF).

[1] E. W. Brooman, *Met. Finish.* **2002**, *100*, 42.
[2] E. W. Brooman, *Met. Finish.* **2002**, *100*, 104.
[3] a) L. S. Kasten, J. T. Grant, N. Grebasch, N. Voevodin, F. E. Arnold, M. S. Donley, *Surf. Coat. Technol.* **2001**, *140*, 11; b) M. Sheffer, A. Groysman, D. Starosvetsky, N. Savchenko, D. Mandler, *Corros. Sci.* **2004**, *46*, 2975; c) M. Garcia-Heras, A. Jimenez-Morales, B. Casal, J. C. Galvan, S. Radzki, M. A. Villegas, *J. Alloys Compd.* **2004**, *380*, 219; d) J. H. Osborne, K. Y. Blohowiak, S. R. Taylor, C. Hunter, G. Bierwagen, B. Carlson, D. Bernard, M. S. Donley, *Prog. Org. Coat.* **2001**, *41*, 217.
[4] A. J. Vreugdenhil, M. E. Woods, *Prog. Org. Coat.* **2005**, *53*, 119.
[5] a) T. G. Shutava, Y. Lvov, *J. Nanosci. Nanotechnol.* **2006**, *6*, 1655; b) V. Kozlovskaya, E. Kharlampieva, M. L. Mansfield, S. A. Sukhishvili, *Chem. Mater.* **2006**, *18*, 328; c) X. F. Yuan, K. Fischer, W. Schärtl, *Langmuir* **2005**, *21*, 9374; d) A. S. Angelatos, B. Radt, F. Caruso, *J. Phys. Chem. B* **2005**, *109*, 3071.
[6] W. Meier, *Chem. Soc. Rev.* **2000**, *29*, 295.
[7] C. Peyratout, H. Möhwald, L. Dähne, *Adv. Mater.* **2003**, *15*, 1722.
[8] S. Förster, T. Plantenberg, *Angew. Chem.* **2002**, *114*, 712; *Angew. Chem. Int. Ed.* **2002**, *41*, 689.
[9] A. Manna, T. Imae, K. Aoi, M. Okada, T. Yogo, *Chem. Mater.* **2001**, *13*, 1674.
[10] A. Sunder, M. Krämer, R. Hanselmann, R. Mülhaupt, H. Frey, *Angew. Chem.* **1999**, *111*, 3758; *Angew. Chem. Int. Ed.* **1999**, *38*, 3552.
[11] G. Schneider, G. Decher, *Nano Lett.* **2004**, *4*, 1833.
[12] D. G. Shchukin, H. Möhwald, *Phys. Chem. Chem. Phys.* **2006**, *8*, 3496.
[13] X. Lu, Z. Xin, *Colloid Polym. Sci.* **2006**, *284*, 1062.
[14] C. I. Zoldesi, C. A. van Walree, A. Imhof, *Langmuir* **2006**, *22*, 4343.
[15] a) A. Harada, K. Kataoka, *Science* **1999**, *283*, 65; b) B. Tan, S. E. Rankin, *Langmuir* **2005**, *21*, 8180; c) H. Djojoputro, X. F. Zhou, S. Z. Qiao, L. Z. Wang, C. Z. Yu, G. Q. Lu, *J. Am. Chem. Soc* **2006**, *128*, 6320.
[16] P. L. Soo, A. Eisenberg, *J. Polym. Sci. Part B* **2004**, *42*, 924.
[17] S. Förster, M. Zisenis, E. Wenz, M. Antonietti, *J. Chem. Phys.* **1996**, *104*, 9956.
[18] B. Jeong, A. Gutowska, *Trends Biotechnol.* **2002**, *20*, 360.
[19] A. D. Bangham, M. M. Standish, J. C. Watkins, *J. Mol. Biol.* **1965**, *13*, 238.
[20] a) M. Iijima, Y. Nagasaki, T. Okada, M. Kato, K. Kataoka, *Macromolecules* **1999**, *32*, 1140; b) Y.-Y. Won, H. T. Davis, F. S. Bates, *Science* **1999**, *283*, 960; c) C. B. Tang, K. Qi, K. L. Wooley, T. Kowalewski, *Angew. Chem.* **2004**, *116*, 2843; *Angew. Chem. Int. Ed.* **2004**, *43*, 2783.
[21] Y. Yoo, D.-C. Kim, T.-Y. Kim, *J. Appl. Polym. Sci.* **1999**, *74*, 2856.
[22] Y. Sun, Y. Li, *J. Colloid Interface Sci.* **2005**, *291*, 7.
[23] D. G. Schukin, E. A. Ustinovich, G. B. Sukhorukov, H. Möhwald, D. V. Sviridov, *Adv. Mater.* **2005**, *17*, 468.
[24] J.-S. Jan, S. Lee, S. Carr, D. F. Shantz, *Chem. Mater.* **2005**, *17*, 4310.
[25] A. M. Collins, C. Spickermann, S. Mann, *J. Mater. Chem.* **2003**, *13*, 1112.
[26] L. Wang, T. Sasaki, Y. Ebina, K. Kurashima, M. Watanabe, *Chem. Mater.* **2002**, *14*, 4827.
[27] a) S. S. Kim, W. Zhang, T. J. Pinnavaia, *Science* **1998**, *282*, 1302; b) D. H. W. Hubert, M. Jung, P. M. Frederik, P. H. H. Bowmans, J. Meuldijk, A. L. German, *Adv. Mater.* **2000**, *12*, 1286; c) Y. Lu, H. Fan, A. Stump, T. L. Ward, T. Reiker, C. J. Brinker, *Nature* **1999**, *398*, 223.
[28] a) M. Jafelicit, Jr., M. R. Davolos, F. Jose de Santos, A. Jose de Santos, *J. Non-Cryst. Solids* **1999**, *247*, 98; b) C. E. Fowler, D. Khushalani, S. Mann, *J. Mater. Chem.* **2001**, *11*, 1968; c) S. Schacht, Q. Huo, I. G. Voigt-Martin, G. D. Stucky, F. Schüth, *Science* **1996**, *273*, 768.
[29] a) R. K. Iler, *J. Colloid Interface Sci.* **1966**, *21*, 569; b) H. Lee, L. J. Kepley, H. G. Hong, S. Akhter, T. E. Mallouk, *J. Phys. Chem.* **1988**, *92*, 2597; c) G. Decher, J.-D. Hong, *Macromol. Symp.* **1991**, *46*, 321.
[30] G. B. Sukhorukov, E. Donath, H. Lichtenfeld, E. Knippel, M. Knippel, A. Budde, H. Möhwald, *Colloids Surf. A* **1998**, *137*, 253.

[31] G. B. Sukhorukov, A. L. Rogach, B. Zebli, T. Liedl, A. G. Skirtach, K. Köhler, A. A. Antipov, N. Gaponik, A. S. Susha, M. Winterhalter, W. J. Parak, *Small* **2005**, *1*, 194.
[32] G. B. Sukhorukov, E. Donath, S. Moya, A. S. Susha, A. Voigt, J. Hartmann, H. Möhwald, *J. Microencapsulation* **2000**, *17*, 177.
[33] G. B. Sukhorukov, M. Brumen, E. Donath, H. Möhwald, *J. Phys. Chem. B* **1999**, *103*, 6434.
[34] G. B. Sukhorukov, A. A. Antipov, A. Voigt, E. Donath, H. Möhwald, *Macromol. Rapid Commun.* **2001**, *22*, 44.
[35] Y. Lvov, A. A. Antipov, A. Mamedov, H. Möhwald, G. B. Sukhorukov, *Nano Lett.* **2001**, *1*, 125.
[36] K. Köhler, D. G. Shchukin, G. B. Sukhorukov, H. Möhwald, *J. Phys. Chem. B* **2005**, *109*,18 250.
[37] M. Sauer, D. Streich, W. Meier, *Adv. Mater.* **2001**, *13*, 1649.
[38] "Sonochemistry and Sonoluminescence": K. S. Suslick, L. A. Crum in *Encyclopedia of Acoustics*, Wiley-Interscience, New York, **1997**, pp. 271 – 282.
[39] J. Rae, M. Ashokkumar, O. Eulaerts, C. von Sonntag, J. Reisse, F. Grieser, *Ultrason. Sonochem.* **2005**, *12*, 325.
[40] a) K. S. Suslick, M. W. Grinstaff, *J. Am. Chem. Soc.* **1990**, *112*, 7807; b) K. S. Suslick, M. W. Grinstaff, K. J. Kolbeck, M. Wong, *Ultrason. Sonochem.* **1994**, *1*, 65.
[41] F. Cavalieri, A. El-Hamassi, E. Chiessi, G. Paradossi, R. Villa, N. Zaffaroni, *Biomacromolecules* **2006**, *7*, 604.
[42] D. G. Shchukin, K. Köhler, H. Möhwald, G. B. Sukhorukov, *Angew. Chem.* **2005**, *117*, 3375; *Angew. Chem. Int. Ed.* **2005**, *44*, 3310.
[43] S. F. Wang, F. Gu, M. K. Lu, *Langmuir* **2006**, *22*, 398.
[44] N. A. Dhas, K. S. Suslick, *J. Am. Chem. Soc.* **2005**, *127*, 2368.
[45] E. Prouzet, F. Cot, C. Boissiere, P. J. Kooyman, A. Larbot, *J. Mater. Chem.* **2002**, *12*, 1553.
[46] E. N. Brown, S. R. White, N. R. Sottos, *J. Mater. Sci.* **2004**, *39*, 1703.
[47] a) R. J. Cardoso, A. Shukla, A. Bose, *J. Mater. Sci.* **2002**, *37*, 603; b) A. M. Zihlif, G. Ragosta, *Polym. Polym. Compos.* **2001**, *9*, 345; c) R. Bagheri, R. A. Pearson, *Polymer* **1996**, *37*, 4529; d) H. S. Kim, M. A. Khamis, *Composites Part A* **2001**, *32*, 1311; e) W. H. Lin, M. H. R. Jen, *J. Compos. Mater.* **1998**, *32*, 1356.
[48] G. Dry, *Compos. Struct.* **1996**, *35*, 263.
[49] X. Liu, J. K. Lee, S. H. Yoon, M. R. Kessler, *J. Appl. Polym. Sci.* **2006**, *101*, 1266.
[50] S. H. Cho, H. M. Andersson, S. R. White, N. R. Sottos, P. V. Braun, *Adv. Mater.* **2006**, *18*, 997.
[51] N. A. Allsop, M. R. Bowditch, N. F. C. Glass, A. E. Harris, P. M. O'Gara, *Thermochim. Acta* **1998**, *315*, 67.
[52] S. Gupta, Q. Zhang, T. Emrick, A. C. Balazs, T. P. Russell, *Nat. Mater.* **2006**, *5*, 229.
[53] S. Lee, M. Müller, R. Heeb, S. Zürcher, S. Tosatti, M. Heinrich, F. Amstad, S. Pechmann, N. D. Spencer, *Tribol. Lett.* **2006**, *24*, 217.
[54] S. Sugama, K. Gawlik, *Mater. Lett.* **2003**, *57*, 4282.
[55] S. H. Li, Q. Liu, J. R. de Wijn, B. L. Zhout, K. de Groat, *Biomaterials* **1997**, *18*, 389.
[56] H. C. Schniepp, D. A. Saville, I. A. Aksay, *J. Am. Chem. Soc.* **2006**, *128*, 12 378.
[57] Z. Li, D. Lee, X. Sheng, R. E. Cohen, M. F. Rubner, *Langmuir* **2006**, *22*, 9820.
[58] L. Zhai, F. C. Cebeci, R. E. Cohen, M. F. Rubner, *Nano Lett.* **2004**, *4*, 1349.
[59] F. C. Cebeci, Z. Wu, L. Zhai, R. E. Cohen, M. F. Rubner, *Langmuir* **2006**, *22*, 2856.
[60] L. Zhai, M. C. Berg, F. C. Cebeci, Y. Kim, J. M. Milwid, M. F. Rubner, R. E. Cohen, *Nano Lett.* **2006**, *6*, 1213.
[61] H. Presting, U. König, *Mater. Sci. Eng. C* **2003**, *23*, 737.
[62] A. A. Voevodin, J. S. Zabinski, *Thin Solid Films* **2000**, *370*, 223.
[63] T. Zhang, D. Y. Lee, *J. Mater. Sci.* **2001**, *36*, 3479.
[64] X. Zhao, Y. Zuo, J. Zhao, J. Xiong, Y. Tang, *Surf. Coat. Technol.* **2006**, *200*, 6846.
[65] H. Masuda, M. Yotsuya, M. Asano, K. Nishio, M. Nakao, A. Yokoo, T. Tamamura, *Appl. Phys. Lett.* **2001**, *78*, 826.
[66] A. Matsuzaki, T. Yamaji, M. Yamashita, *Surf. Coat. Technol.* **2003**, *169–170*, 655.
[67] G. Hultquist, B. Tveten, E. Hörnlund, M. Limbäck, R. Haugsrud, *Oxid. Met.* **2001**, *56*, 313.
[68] Y. J. Tan, S. Bailey, B. Kinsella, *Corros. Sci.* **1996**, *38*, 1545.
[69] G. Paliwoda-Porebska, M. Stratmann, M. Rohwerder, K. Potje-Kamloth, Y. Lu, A. Z. Pich, H.-J. Adler, *Corros. Sci.* **2005**, *47*, 3216.
[70] M. Kendig, M. Hon, L. Warren, *Prog. Org. Coat.* **2003**, *47*, 183.
[71] K. Aramaki, *Corros. Sci.* **2005**, *47*, 1285.
[72] K. Aramaki, *Corros. Sci.* **2006**, *48*, 3298.
[73] a) K. Aramaki, *Corros. Sci.* **2003**, *45*, 2361; b) K. Aramaki, *Corros. Sci.* **2003**, *45*, 451; c) S. X. Yu, Z. W. Zhang, L. Chen, J. Han, *J. Rare Earths* **2005**, *23*, 255.
[74] a) M. L. Zheludkevich, I. M. Salvado, M. G. S. Ferreira, *J. Mater. Chem.* **2005**, *15*, 5099; b) A. N. Khramov, N. N. Voevodin, V. N. Balbyshev, M. S. Donley, *Thin Solid Films* **2004**, *447–448*, 549.
[75] N. N. Voevodin, N. T. Grebasch, W. S. Soto, F. E. Arnold, M. S. Donley, *Surf. Coat. Technol.* **2001**, *140*, 24.
[76] M. L. Zheludkevich, R. Serra, M. F. Montemor, M. G. S. Ferreira, *Electrochem. Commun.* **2005**, *7*, 836.
[77] S. V. Lamaka, M. L. Zheludkevich, K. A. Yasakau, M. F. Montemor, P. Cecilio, M. G. S. Ferreira, *Electrochem. Commun.* **2006**, *8*, 421.
[78] Y. M. Abu, K. Aoki, *J. Electroanal. Chem.* **2005**, *583*, 133.
[79] M. Tomalino, G. Bianchini, *Prog. Org. Coat.* **1997**, *32*, 17.
[80] C. Schmidt, US patent 6,383,271 "Anti-corrosive coating including a filler with a hollow cellular structure", 7 May, **2002**.
[81] R. L. Cook, US patent 6,933,046 "Releasable corrosion inhibitor compositions", 23 August, **2005**.
[82] a) W. M. Sutherland, US patent 3,899,624 "Method for protecting surfaces against environmental damage and the resultant products", 12 August, **1975**; b) P. E. Eckler, L. M. Ferrara, US patent 4,738,720 "Anticorrosive protective coatings", 19 April, **1988**; c) D. A. Pippard, US patent 4,405,493 "Corrosion inhibitors, method of producing them and protective coatings containing them" 20 September, **1983**.
[83] a) D. G. Shchukin, M. L. Zheludkevich, K. A. Yasakau, S. V. Lamaka, M. G. S. Ferreira, H. Möhwald, *Adv. Mater.* **2006**, *18*, 1672; b) M. L. Zheludkevich, D. G. Shchukin, K. A. Yasakau, H. Möhwald, M. G. S. Ferreira, *Chem. Mater.* **2007**, *19*, 402; c) D. G. Schukin, H. Möhwald, Adv. Funct. Mater. 2007, in press, DOI: 10.1002/adfm.200601226; d) D. G. Schukin, M. L. Zheludkevich, H. Möhwald, *J. Chem. Mater.* **2006**, *16*, 4561.

Received: January 25, 2007
Published online on April 26, 2007

